

This manuscript is submitted for publication in Renewable and Sustainable Energy Reviews. Please note that, this manuscript has not undergone peer-review and is not yet formally accepted for publication. Subsequent versions of this manuscript may have slightly different content.

Storage Integrity during Underground Hydrogen Storage in Depleted Gas Reservoirs

Zeng, L.^{1*}, Sarmadivaleh, M.¹, Saeedi, A.¹, Chen, Y.², Zhong, Z.³ and Xie, Q.¹

¹*WA School of Mines: Minerals, Energy and Chemical Engineering, Curtin University, 26 Dick Perry Avenue, Kensington, WA, 6151, Australia*

²*Department of Chemical Engineering and Analytical Science, University of Manchester, Manchester, UK*

³*College of Energy, Chengdu University of Technology, Chengdu, China*

* = Corresponding author details, Lingping.zeng@curtin.edu.au

Abstract

The transition of energy from fossil fuels to renewable energy particularly hydrogen is becoming the centre of decarbonization and roadmap to achieve net-zero carbon emission. To meet the requirement of large-scale hydrogen storage as a key part of hydrogen supply chain, underground hydrogen storage can be the ultimate solution to economically store hydrogen thus meet global energy demand. Compared to other types of subsurface storage sites such as salt caverns and aquifers which are limited to geographical locations, depleted gas reservoirs have been raising more interest because of the wider distribution and higher storage capacity. However, safely storing and cycling of hydrogen in depleted gas reservoirs requires caprock, reservoir and wellbore to remain high stability and integrity. Nevertheless, current research on storage integrity during underground hydrogen in depleted gas reservoirs is still scarce and non-systemic. We therefore reviewed the major challenges on storage integrity associated with geochemical reactions, microbial activities, faults and fractures and

hydrogen cycling perspectives. The processes and impacts of abiotic and biotic mineral dissolution/precipitation, faults and fracture reactivation and propagation in caprock and host-rock, wellbore instability due to cement degradation and casing corrosion, stress change during hydrogen cycling, etc. on storage integrity were comprehensive reviewed and analysed. Furthermore, a technical screening tool with consideration of controlling variables, risks and consequences on storage integrity was developed to identify the potential risks associated with storage integrity. Lastly, knowledge gaps together with feasible methods and pathways have been identified to mitigate the risks and thus enables large-scale underground hydrogen storage.

Keywords: Underground hydrogen storage, Storage integrity, Geochemical reactions, Microbial activities, Hydrogen cycling, Technical screening tool.

Word Count: 15823 words (references excluded)

1. Introduction

While fossil fuel is the backbone of current energy structure [1], the supply of petroleum suffers from war and long-distance transport. Moreover, the usage of fossil fuel is creating emerging environmental concerns [2]. Raised climate goals and rebounding economy are driving renewable energy to new records [3]. IEA predicted that the renewable energy would account for 95% of global power increase by 2026 [4]. Among the renewable energy, solar energy and wind power are the powerhouse in global energy market, which are predicted to reach over 50% of power supply [4]. Therefore, renewable energy is crucial to achieve any energy transition and thus reach net zero [5].

However, the main drawbacks of renewable energy include seasonal, intermittent, and geographical constrained supply [6-8]. The unsteady nature of weather and uneven distribution of energy farms bring on fluctuating power generation [9]. The unstable characters of renewable energy renders varying supply of electricity [10], which results in energy excesses and deficits [11, 12]. To alleviate these drawbacks and promote large-scale deployment of renewable energy, an efficient, reliable, scalable, and economic energy storage system is critical in the form of hydrogen [9]. This is mainly because hydrogen appears to be a great energy carrier due to its high energy density and zero emission [13].

To store the extra generated hydrogen, large-scale hydrogen storage facility was brought forward to achieve large scale and scalable energy storage method [14]. Two hydrogen storage roadmaps have been considered: surface hydrogen storage and underground hydrogen storage (UHS). Surface hydrogen storage methods include physical storage and chemical storage [15, 16]: i) Physical methods incorporate compressed, liquefied or cryo-compressed hydrogen in

pressured vessels [17]. ii) Chemical methods employ materials-based reactions, such as hydrogen sorption in metal or organic matters [18]. Substantial advances have been achieved in chemical hydrogen storage methods in recent years. However, the safety issues, limited space, and high cost increase the height of hurdles for large-scale applications of surface hydrogen storage [19] (both physical and chemical storage methods).

To enable large-scale hydrogen storage in the renewable era, the UHS has been the centre of attention for its low cost and scalable character [8, 16, 20]. Besides, hydrogen storage in subsurface reservoirs appears to be safe and with huge storage capacity (orders of magnitude larger than surface storage methods) [1, 20]. The potential subsurface sites are salt caverns, saline aquifers, and depleted hydrocarbon fields [21]. As reported in literature, ten UHS projects are under operation (Table 1 [1]), indicating UHS as a prospective technology for large-scale and long-term storage. The typical capacity of a reservoir for UHS ranges to billions of m³ with cost further lowered with increasing hydrogen cycling times [22]. UHS is thus regarded as one of the pillars for future hydrogen market chain.

Although the UHS is an attracting future energy solution [14, 16, 23, 24], the UHS is indeed associated with certain risks and uncertainties [25]. For example, one of the major uncertainties rises from storage integrity, which links to the integrity of caprock, wellbore, and reservoir [5]. Caprock integrity involves wetting alteration of caprock [26-28], reduction of geo-mechanical strength, and fault reactivation [29, 30]. Wellbore integrity face challenges of extreme temperature change and fluctuating pressure during gas cycling flow process [31]. Reservoir integrity is determined by geochemical reactions (e.g. dissolution reactions [19] and fluid-rock interfacial reactions [32, 33]) and microbial activities, which affect rock surface wetting, traps and limits hydrogen flow in porous media. Recent excellent reviews have outlined the advances and trend of UHS technology [5, 15, 21, 26, 34, 35]. However, few reviews have focused on the storage integrity. Given that the critical role of storage integrity in UHS, we identified and evaluated the governing factors and its evolution in underground reservoirs during UHS. This review focused on recent advances of in geochemical reactions and microbial activities and their implications on storage integrity.

Region	Project	Location	Period	Developer		Funding Resources	Type	Impacts
UK	HyStorPor[37]	Edinburgh	2019-2023	Scotland Gas Network Pale Blue Dot Scottish Hydrogen & Fuel Cell Asso SHFCA	University of Edinburgh	Industry	Porous rocks	<ol style="list-style-type: none"> 1. Engage opinion-shaping citizens in dialogue on how hydrogen storage may affect daily living. 2. Assist the nascent hydrogen energy industry by providing developers with scientific understanding of commercial hydrogen storage in the subsurface. 3. Benefit the international academic community by furthering scientific understanding of geological hydrogen storage in the areas of reactivity and multiphase flow.
	Teeside[38]	North East England	1972	Sabir Petrochemicals	NA	NA	Bedded salt	<ol style="list-style-type: none"> 1. With 210,000 m³ geometrical volume that could store 27GWT H₂. 2. Storage capacity is limited but costly.
US	Moss Bluff[39]	Texas	2007	Praxair	NA	Industry	Salt dome	Praxair's Gulf Coast pipeline network has the capability of supplying 600 million cubic feet per day (16 million cubic meters per day) of hydrogen on a steady-state basis, with peaking capacity of 700 million cubic feet per day (18 million cubic meters per

Region	Project	Location	Period	Developer		Funding Resources	Type	Impacts
								day).
	Spindletop[40]	Texas	2017	Air Liquide	NA	NA	Salt dome	<p>1. With 906,000 m³ geometrical volume that could store 274GWT H₂.</p> <p>2. It is of great benefit to have a large, interconnected storage solution to optimize supply to customers reliably and efficiently.</p> <p>3. Hydrogen is used in the refining process to desulfurize fuels and in several other industrial and manufacturing processes.</p>
	ConocoPhillips Clemens Terminal[41]	Texas	1983	ConocoPhillips and Praxair	NA	Industry		<p>1. Costs for underground hydrogen storage are about 2 orders of magnitude lower than those for other forms of hydrogen storage (high-pressure cylinders, etc.)</p> <p>2. The characteristics of the bulk storage system will drive the characteristics of much of the hydrogen economy, including the likely roles of nuclear hydrogen relative to other methods of hydrogen production.</p>
EU	Hyunder[42]	France Germany Netherlands Romania	2013	Fundación Hidrógeno Aragón CENEX	NA	Industry & Government	salt caverns	<p>1. A need for further assessment has been identified whether it will be possible to improve</p>

Region	Project	Location	Period	Developer		Funding Resources	Type	Impacts
		Spain the United Kingdom (UK).		CEA DEEP ECN E.ON Hinicio LBST KBB National Hydrogen and Fuel Cell Centre Shell Solvay				<p>the business case for electrolysis in the short to medium term.</p> <p>2. Hands-on operational experience and demonstration in preparation of future markets are needed.</p> <p>3. Incentivizing the construction of hydrogen caverns for these applications would put the required infrastructure in place</p> <p>4. All options and all markets need favourable policy and regulatory frameworks with high level of continuity, to reduce early investment risks.</p>
	Underground Sun Storage[43]	Pilsbach, Upper Austria	2013	RAG Austria AG Axiom Energy Institute at the JKU Linz Verbund	University of Leoben University of Natural Resources and Applied Life Sciences	Industry	porous Rocks	<p>1. The provision of large-volume and seasonal storage facilities is a key challenge in the conversion of our energy production to renewable fluctuating sources.</p> <p>2. There is still a need for research in the field of geochemistry and in particular on the solubility of hydrogen in reservoir water.</p> <p>3. Both the integrity of the storage facilities and the field test with the</p>

Region	Project	Location	Period	Developer		Funding Resources	Type	Impacts
								associated facilities were sufficiently confirmed over a period of four years.
	Vienna Basin Green Hydrogen (H ₂) Storage Project[44]	Gaiselberg and Zistersdorf, Austria	2021	ADX Energy Ltd and Horváth	NA	NA	Porous rocks	<ol style="list-style-type: none"> To evaluate the deployment of reservoirs at the Gaiselberg and Zistersdorf producing fields in the Vienna Basin (ADX Fields) for green hydrogen (H₂) storage. ADX can build the subsurface energy storage facility for a tenth of the Tesla battery cost and 2.5 times cheaper.
	MefHySto Project[45]	EU	2019	European Metrology Programme on Innovation and Research (EMPIR) and consists of 14 consortium partners from all over Europe	NA	NA	NA	<ol style="list-style-type: none"> Assess the quality of hydrogen produced and improve the reference equations of state used for modelling hydrogen injection. The project will investigate the sustainability and reliability of fuel cells (FC), whose performance is affected by impurities in hydrogen and develop a harmonized method for hydrogen storage. The project will deal with metrological and thermodynamic issues in the large-scale storage of hydrogen in underground

Region	Project	Location	Period	Developer		Funding Resources	Type	Impacts
								gas storages (UGS) and the conversion of existing UGS from natural gas to hydrogen.
	Large-Scale Energy Storage in Salt Caverns and Depleted Gas Fields[46, 47]	Netherlands	2019	TNO EBN Gasunie Gasterra NAM Nouryon	NA	Industry	Salt Cavern	<ol style="list-style-type: none"> 1. Analysis of the role of large-scale storage in the future energy system. 2. Techno-economic modelling (performance, cost, economics) of large-scale energy storage systems, focusing on CAES and UHS in salt caverns, and UHS in depleted gas fields - analogous to UGS. 3. Assessment of the current policy and regulatory frameworks and how they limit or support the deployment of large-scale energy storage, and stakeholder perception regarding energy storage. 4. Risk identification and screening for the selected large-scale subsurface energy storage technologies.

2. Characteristics of hydrogen

2.1 Hydrogen physical properties

Understanding fundamental properties of hydrogen is in favour of the design and operation of underground hydrogen storage, and thus de-risks the potential concerns on storage integrity. Considering the underground gas storage has been widely used to store natural gas to manage the energy supply chain [48-51] and carbon dioxide to reduce carbon emissions (which is known as CO₂ geosequestration or carbon capture and storage, CCS) [52-54], it is worthwhile to compare the physical properties of hydrogen with CH₄ and CO₂ (Table 2). H₂ has a higher heating value or energy density per mass (120-141.8 MJ/kg) compared to hydrocarbon, which makes it a perfect fuel as energy carrier. However, the less heating value per volume (10.8-12.7 MJ/m³ compared to CH₄ which is 35.8-39.8 MJ/m³) implies that the tremendous volume of space is a must to store H₂. Given the low critical temperature and pressure of hydrogen, H₂ would be stored in the form of gas phase in subsurface [55], which is the natural advantage of depleted gas reservoirs due to their enormous storing spaces and high availability compared to other UHS sites particularly the salt caverns and saline aquifers [56-58]. Meanwhile, the cycling of gas phase H₂ combined pre-injected cushion gas and *in-situ* formation brine leads to complex multiphase flow behavior, requesting more complex equation of states (EOS) to characterize the flow patterns and properties [59].

Table 2 Comparison of physical properties among H₂, CO₂ and CH₄ [5, 60, 61].

Variables	H ₂	CO ₂	CH ₄
Molecular weight (g/mol)	2.016	44.01	16.043
Density at 298 K and 0.1 MPa (kg/m ³)	0.082	1.98	0.657
Viscosity at 298 K and 0.1 MPa (Pa·s)	8.9×10^{-6}	1.48×10^{-5}	1.1×10^{-5}
Critical pressure (MPa)	1.297	7.377	4.640

Critical temperature (K)	33.20	304.13	190.8
Mass heating value (MJ/kg)	120-141.8	n/a	50-55.5
Volumetric heating value (MJ/m ³)	10.8-12.7	n/a	35.8-39.8
Solubility in pure water at 298 K and 0.1 MPa (mol/kgw)	7.9×10^{-4}	0.033	1.4×10^{-3}
Diffusion in pure water at 298 K (m ² /s)	5.13×10^{-9}	1.6×10^{-9}	1.85×10^{-9}

Hydrogen is much less dense than CO₂ and CH₄. Therefore, the storage of same mass of H₂ requires more pressure and once again calls for the importance of storage capacity [5, 62]. Besides, the low density of H₂ leads to an accumulated hydrogen cap below caprock, which serves as a geologic seal for H₂ from escaping the storage site [63]. The denser cushion gas, e.g., CH₄ or N₂, would gather around H₂ in the form of cushion gas plume to maintain enough formation pressure during H₂ withdrawn process.

The viscosity of hydrogen is also less than CO₂ and CH₄, implying a higher hydrogen mobility. Therefore, it could be expected lower residual hydrogen trapped in subsurface and higher reproduction efficiency [5]. Besides, viscosity also partly determines the water coning effect during conventional hydrocarbon production, where the interface between gas/oil and underlying water gradually moves upward and bears productivity [64, 65]. The less viscosity of hydrogen is helpful to suppress the water coning issues [66]. On the other hand, the low viscosity of hydrogen could also induce the viscous fingering since hydrogen is unlikely displacing formation brine uniformly, leading to a certain amount of unrecoverable hydrogen [67]. Changing pressure and temperature within the range of typical geological conditions has very limited effect on hydrogen viscosity (variation in the range of 9 to 11×10^{-6} Pa·s at pressure of 0.1 to 50 MPa and temperature of 25 to 120 °C [36]). Consequently, the relatively stable of hydrogen viscosity is conducive to simplification of the calculation of EOS and multiphase flow behavior among stored H₂, surrounding cushion gas and pre-existing formation brine.

2.2 Hydrogen solubility and dissociation in saline brines

During the underground hydrogen storage, the injected hydrogen directly contacts with formation brine. Therefore, understanding the solubility of hydrogen is of vital importance when storing hydrogen in subsurface porous media for the monitoring and optimization of hydrogen mobility and reactivity. As a non-polar gas, hydrogen is hardly dissolved in water. At temperature of 298 K and standard atmospheric pressure condition, the solubility of hydrogen in pure water is around 7.9×10^{-4} mol/kgw [68, 69], which is slightly lower than CH₄ with 1.4×10^{-3} mol/kgw [70], but much lower than CO₂ with more than one order of magnitude (0.033 mol/kgw [71]). Hydrogen solubility increases with increasing pressure, but decreases with increasing temperature and salinity [68, 72]. Bo et al. [19] simulated the hydrogen solubility in saline brines with different salinities. The results show that at constant pressure and temperature conditions, increasing salinity from 5,000 to 35,000 ppm slightly decreases the hydrogen solubility of approximately 1×10^{-4} mol/kgw. Similar results are reported by Wiesenburg and Guinasso [68], and Chabab et al. [73]. Overall, the extremely low solubility of hydrogen in saline brines indicates a negligible amount of hydrogen loss due to the hydrogen dissolution during UHS.

Given the high stability of hydrogen molecules, the dissociation of aqueous hydrogen in saline brines without minerals involved would be extremely weak. According to the thermodynamic data from WATEQ4F database associated within geochemical solver PHREEQC [74], the aqueous H₂ dissociation is defined by:



Where $\log K_{298\text{k}}$ is -3.15 and enthalpy is -1.759 kJ/mol.

Noting that the phase of hydrogen in Eq. 1 is dissolved hydrogen, which means that the gas phase hydrogen needs to dissolve into formation brine first, and the reaction is defined in Lawrence Livermore National Laboratory database (LLNL, thermo.com.V8.R6.230) [74] by:



Where $\log K_{298\text{k}}$ is -3.105 and enthalpy is -4.184 kJ/mol.

Considering the low solubility of hydrogen, the hydrogen loss caused by the further dissociation without presence of minerals should be negligible. However, the host rock of hydrogen plays a significant role in UHS, not only because of the petrophysical properties such as porosity, permeability and connectivity that

affects the hydrogen cycling, but also that hydrogen can react with some sensitive minerals (e.g., calcite, dolomite, siderite, pyrite, etc.) through redox reactions (the dissociation of hydrogen is actually an oxidation process as one of the half reactions of the redox; see detailed discussion in section 3.1.1). In this case, the dissociation of hydrogen would be facilitated, leading to considerable volume of hydrogen loss and minerals dissolution thus umpiring the stability and integrity of caprock and host rock in reservoirs.

2.3 Hydrogen diffusivity

The low molecular weight of hydrogen makes it more diffusive than other gases. In pure water at 298 K and standard pressure, the diffusion coefficient of hydrogen is around $5.13 \times 10^{-9} \text{ m}^2/\text{s}$ [75], where only 1.6×10^{-9} and $1.85 \times 10^{-9} \text{ m}^2/\text{s}$ for CO_2 [76] and CH_4 [77]. The impact of hydrogen diffusivity can be classified into two categories: upward diffusion through caprock and interphase diffusion into other *in-situ* fluids. The upward diffusion through caprock even overburdens could lead to extra hydrogen loss. Due to the presence of minerals, the diffusion coefficient in porous media needs to be scaled with tortuosity by considering porosity to represent the effective diffusion coefficient [78]. For the interphase diffusion, it mainly causes the mixing of stored hydrogen with pre-injected cushion gas or residual natural gas and results in hydrogen contamination, and thus the cycling efficiency and withdrawn recovery [79], which is beyond the scope of this work (the storage integrity).

3. Geochemical reactions

When hydrogen is injected into subsurface porous media, it can react with certain types of minerals which are usually sensitive to redox reactions, leading to mineral dissolution/precipitation. The comprehensive geochemical reactions among stored hydrogen, formation brine and minerals would affect the storage integrity and stability. For caprock, the geochemical process between hydrogen and sensitive minerals could affect the porosity and permeability which are highly related to the sealing capacity. Besides, the wettability, capillary pressure and hydrogen upward diffusion are also governed by the physicochemical properties of caprock, affecting the long-term trapping ability and containment on hydrogen. For reservoirs, the mineral dissolution and precipitation would influence the formation connectivity and fluid migration, thus the hydrogen cycling efficiency and ultimate withdrawn recovery. Furthermore, the geochemical reactions can change the *in-situ* brine geochemistry, which in turn affects the geochemical reactions and abiotic hydrogen loss. On the other hand, the mineral dissolution and precipitation taking place at near wellbore area would significantly umpire the stability of wellbore and trigger borehole collapse and failure. Moreover, the cement degradation induced by the geochemical reactions with surrounding hydrogen can also cause the wellbore instability thus

affecting productivity. In this section, we will review and summarize the primary controlling factors of geochemical reactions in caprock, reservoirs and wellbore.

3.1 Caprocks

3.1.1 Role of sensitive minerals

The geochemical reactions between stored hydrogen and caprock in the presence of *in-situ* brine may lead to mineral dissolution or precipitation, and affect the caprock porosity, permeability and connectivity thus the sealing capacity to prevent hydrogen from migrating upward. The mineral dissolution induced by geochemical reactions could also affect the caprock mechanical properties so as the overall integrity and stability during hydrogen cycling. Therefore, it is important to characterize the effect of geochemical reactions within caprock to assess its long-term integrity during UHS projects. Current geochemical modelling on mineral dissolution/precipitation mainly consists of two types: thermodynamic modelling and kinetic modelling [19, 59, 80-83]. The thermodynamic or equilibrium modelling only calculates the ultimate extent of mineral reactions in an infinite time scale. Hence, it often overestimates the degree of mineral dissolution or precipitation [36]. Kinetic batch modelling and reactive transport modelling account for the mineral reaction rates and can estimate the time-dependent mineral dissolution/precipitation. However, the key input parameters, including the kinetic rate constant, Arrhenius activation energy and reaction order at acid, neutral and base mechanism used for UHS need to be calibrated from H₂ associated experiment to improve the prediction accuracy [59]. This is also true for the equilibrium modelling, where the databases covering equilibrium reaction constants and enthalpy for individual mineral reactions also need to be updated. Table 3 and 4 list the reactions and the core input parameters for equilibrium modelling and kinetic modelling on carbonates, sulfates, sulfide (pyrite) and Fe³⁺-bearing minerals from the widely used geochemical database. These minerals are highlighted because that they are identified as the sensitive minerals during UHS since they can react with injected H₂ through redox process. Therefore, the dissolution/precipitation more likely take place in the caprock rich in these sensitive minerals and thus affect the caprock integrity and sealing capacity.

Table 3 Thermodynamic non-reductive dissolution (from LLNL database [74]) and reductive dissolution of identified sensitive minerals.

Minerals	Non-reductive dissolution	Reductive dissolution
<u>Carbonates</u>		

Calcite	$\text{CaCO}_3 + \text{H}^+ = \text{Ca}^{2+} + \text{HCO}_3^-$	$\text{CaCO}_3 + 4\text{H}_2 = \text{Ca}^{2+} + \text{CH}_4 + 2\text{OH}^- + \text{H}_2\text{O}$
Dawsonite	$\text{NaAlCO}_3(\text{OH})_2 + 3\text{H}^+ = \text{Al}^{3+} + \text{Na}^+ + \text{HCO}_3^- + 2\text{H}_2\text{O}$	$\text{NaAlCO}_3(\text{OH})_2 + 4\text{H}_2 = \text{Al}^{3+} + \text{Na}^+ + \text{CH}_4 + 4\text{OH}^- + \text{H}_2\text{O}$
Dolomite ^a	$\text{CaMg}(\text{CO}_3)_2 + 2\text{H}^+ = \text{Ca}^{2+} + \text{Mg}^{2+} + 2\text{HCO}_3^-$	$\text{CaMg}(\text{CO}_3)_2 + 8\text{H}_2 = \text{Ca}^{2+} + \text{Mg}^{2+} + 2\text{CH}_4 + 4\text{OH}^- + 2\text{H}_2\text{O}$
Dolomite ^b	$\text{CaMg}(\text{CO}_3)_2 + 2\text{H}^+ = \text{Ca}^{2+} + \text{Mg}^{2+} + 2\text{HCO}_3^-$	$\text{CaMg}(\text{CO}_3)_2 + 8\text{H}_2 = \text{Ca}^{2+} + \text{Mg}^{2+} + 2\text{CH}_4 + 4\text{OH}^- + 2\text{H}_2\text{O}$
Magnesite	$\text{MgCO}_3 + \text{H}^+ = \text{HCO}_3^- + \text{Mg}^{2+}$	$\text{MgCO}_3 + 4\text{H}_2 = \text{Mg}^{2+} + \text{CH}_4 + 2\text{OH}^- + \text{H}_2\text{O}$
Siderite	$\text{FeCO}_3 + \text{H}^+ = \text{Fe}^{2+} + \text{HCO}_3^-$	$\text{FeCO}_3 + 4\text{H}_2 = \text{Fe}^{2+} + \text{CH}_4 + 2\text{OH}^- + \text{H}_2\text{O}$
<u>Sulfates</u>		
Anglesite	$\text{PbSO}_4 = \text{Pb}^{2+} + \text{SO}_4^{2-}$	$\text{PbSO}_4 + 4\text{H}_2 = \text{Pb}^{2+} + \text{H}_2\text{S} + 2\text{OH}^- + 2\text{H}_2\text{O}$
Anhydrite	$\text{CaSO}_4 = \text{Ca}^{2+} + \text{SO}_4^{2-}$	$\text{CaSO}_4 + 4\text{H}_2 = \text{Ca}^{2+} + \text{H}_2\text{S} + 2\text{OH}^- + 2\text{H}_2\text{O}$
Gypsum	$\text{CaSO}_4 \cdot 2\text{H}_2\text{O} = \text{Ca}^{2+} + \text{SO}_4^{2-} + 2\text{H}_2\text{O}$	$\text{CaSO}_4 \cdot 2\text{H}_2\text{O} + 4\text{H}_2 = \text{Ca}^{2+} + \text{H}_2\text{S} + 2\text{OH}^- + 4\text{H}_2\text{O}$
Barite	$\text{BaSO}_4 = \text{Ba}^{2+} + \text{SO}_4^{2-}$	$\text{BaSO}_4 + 4\text{H}_2 = \text{Ba}^{2+} + \text{H}_2\text{S} + 2\text{OH}^- + 2\text{H}_2\text{O}$
Celestite	$\text{SrSO}_4 = \text{SO}_4^{2-} + \text{Sr}^{2+}$	$\text{SrSO}_4 + 4\text{H}_2 = \text{Sr}^{2+} + \text{H}_2\text{S} + 2\text{OH}^- + 2\text{H}_2\text{O}$

<u>Sulfide</u>		
Pyrite	$\text{FeS}_2 + \text{H}_2\text{O} = 0.25\text{H}^+ + 0.25\text{SO}_4^{2-} + \text{Fe}^{2+} + 1.75 \text{HS}^-$	$\text{FeS}_2 + \text{H}_2 = \text{FeS} + \text{H}_2\text{S}$
<u>Fe³⁺ Oxides</u>		
Goethite	$\text{FeO}(\text{OH}) + 3\text{H}^+ = \text{Fe}^{3+} + 2\text{H}_2\text{O}$	$2\text{FeO}(\text{OH}) + \text{H}_2 = 2\text{Fe}(\text{OH})_2$
Hematite	$\text{Fe}_2\text{O}_3 + 6\text{H}^+ = 2\text{Fe}^{3+} + 3\text{H}_2\text{O}$	$\text{Fe}_2\text{O}_3 + \text{H}_2 + \text{H}_2\text{O} = 2\text{Fe}(\text{OH})_2$

^aSedimentary (disordered) dolomite.

^bHydrothermal (ordered) dolomite.

Table 4 Input parameters for kinetic reactions of sensitive minerals (data from Palandri and Kharaka [84]). $\log k_{298\text{K}}$ represents the log of reaction rate constant, E_a is Arrhenius activation energy, kJ/mol, n is reaction order and M is mineral molar mass, g/mol.

Minerals	Acid mechanism			Neutral mechanism		Base mechanism			M (g/mol)
	$\log k_{298\text{K}}$	E_a (kJ/mol)	n	$\log k_{298\text{K}}$	E_a (kJ/mol)	$\log k_{298\text{K}}$	E_a (kJ/mol)	n	
<u>Carbonates</u>									
Calcite	-0.3	14.4	1	-5.81	23.5	-3.48	35.4	1	100.09
Dawsonite	-	-	-	-7	62.8	-	-	-	144
Dolomite ^a	-3.19	36.1	0.5	-7.53	52.2	-5.11	34.8	0.5	184.4

Dolomite ^b	-3.76	56.7	0.5	-8.6	95.3	-5.37	45.7	0.5	184.4
Magnesite	-6.38	14.4	1	-9.34	23.5	-5.22	62.8	1	84.31
Siderite [85]	-11.75	54.5	0.75	-	-	-	-	-	115.854
<u>Sulfates</u>									
Anglesite	-5.58	31.3	0.298	-6.5	31.3	-	-	-	303.26
Anhydrite	-	-	-	-3.19	14.3	-	-	-	138.16
Gypsum	-	-	-	-2.79	0	-	-	-	172.2
Barite	-6.9	30.8	0.22	-7.9	30.8	-	-	-	233.39
Celestite	-5.66	23.8	0.109	-	-	-	-	-	183.68
<u>Sulfide</u>									
Pyrite	-7.52	56.9	0.5 ^c	-4.55	56.9	-	-	-	119.98
<u>Fe³⁺ Oxides</u>									
<u>Goethite</u>	-	-	-	-7.94	86.5	-	-	-	88.85
Hematite	-9.39	66.2	1	-14.6	66.2	-	-	-	159.688

^aSedimentary (disordered) dolomite.

^bHydrothermal (ordered) dolomite.

^cReaction order n with respect to Fe³⁺; -0.5 if it is with respect to H⁺

3.1.1.1 Carbonates

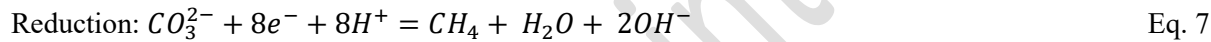
The hydrogen induced carbonates dissolution at typical reservoir temperature and pressure conditions can only occur with participation of formation brine, where the aqueous hydrogen reacts with dissolved carbonate minerals (CO_3^{2-} and HCO_3^-) and generates CH_4 through the redox. At dry conditions, so far there is no direct evidence from experiments showing that H_2 could reduce C(4) from carbonate minerals, except for the extremely high temperature condition (for example, 535 to 870 °C [86]) which is unrealistic in common depleted gas reservoirs. The geochemical reactions between stored hydrogen mainly consists of three steps. Taking calcite for example. First, calcite dissolves into formation brine which is given by:



Meanwhile, the gas phase H_2 dissolves into brine and equilibrates with aqueous phase through the Eq. 2 defined in the section 2.2. Then, the generated CO_3^{2-} and HCO_3^- are reduced by aqueous H_2 and form CH_4 through the redox reaction. For CO_3^{2-} , it is given by:



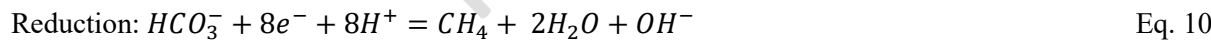
which can be further separated into two half-reactions:



For HCO_3^- , it is given by:



where the two half-reactions are given by:



In general, the C(4) within $\text{CO}_3^{2-}/\text{HCO}_3^-$ acting the role of e^- receiver is reduced by H_2 which is e^- donor and form CH_4 . The redox reactions between $\text{CO}_3^{2-}/\text{HCO}_3^-$ and aqueous H_2 in turn facilitate the dissolution of calcite and other carbonate minerals. For calcareous shale caprock which is rich in calcite, the redox reactions between calcite and stored hydrogen would lead to calcite dissolution, compromising the matrix of calcareous shale and weakening the caprock integrity. For siliceous and argillaceous shale caprocks where carbonates take less proportion, the hydrogen induced carbonate dissolution may impair the carbonate cementation [87, 88], which also affects the caprock integrity and long-term sealing capacity. The observations on carbonates dissolution during UHS from geochemical modelling are reported by Amid et al. [89], Bo et al. [19], Hassannayebi et al. [59], Hemme and Van Berk [81], Pichler [90] and Zeng et al. [91]. In terms of experiments, Pudle et al. [92] evaluated the geochemical processes within sandstone samples containing certain amounts of carbonates from Europe and Argentina. The samples were exposed to hydrogen at pressure of 4 to 20 MPa, temperature of 40 to 120 °C and salinity of 16,000 to 350,000 mg/L. They compared the samples' properties through petrophysical, tomographic, mineralogical and geochemical methods before and after hydrogen treatment. They found no evidence of minerals reactions at low pressure, temperature and salinity conditions. However, at higher pressure, temperature and salinity conditions, calcite partially to totally dissolved. Similar results were reported by Bensing et al. [93, 94], who observed a significant dissolution of calcite fragments in claystone caprock that were saturated with hydrogen and 10 wt% NaCl solution.

3.1.1.2 Sulfates

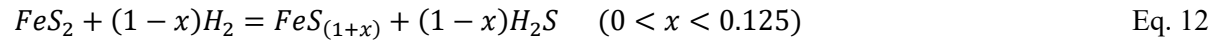
For sulfate minerals, the stored hydrogen can reduce SO_4^{2-} from anglesite (PbSO_4), anhydrite (CaSO_4), gypsum ($\text{CaSO}_4 \cdot 2\text{H}_2\text{O}$), barite (BaSO_4) and celestite (SrSO_4) to H_2S through the redox reaction:



The generate H_2S can either form gas phase or dissolve as aqueous phase due to its high solubility [95] and further dissociate to HS^- and S^{2-} . Similar to carbonate minerals, the dissolution of sulfate minerals could partially affect the caprock integrity and rock mechanical behaviours [96]. The sulfate minerals dissolution induced by redox reactions with hydrogen is reported by Hemme and Van Berk [81] and Lassin et al. [97] from geochemical simulation. From experiment point of view, Pudle et al [92], Henkel et al. [98] and Flesch et al. [99] observed the dissolution of sulfates (typically anhydrite and barite) in sandstones when exposed to hydrogen and saline brine. Similar results were also reported by Truche et al. [100, 101] and Cozzarelli et al. [102].

3.1.1.3 Sulfide

As a sulfide mineral, pyrite (FeS_2) can be reduced by stored hydrogen and generate pyrrhotite or troilite (FeS) through the reaction [59, 103, 104]:



Truche et al. [103] studied the kinetics of pyrite to pyrrhotite reduction in the presence of hydrogen and 27 mM NaCl and calcite-buffered solution at temperature between 90 and 180 °C and hydrogen partial pressure between 0-18 bar. They observed a partial reduction of pyrite by hydrogen to pyrrhotite, which was caused by the interactions between substrate-mediated pyrrhotite nucleation and solution chemistry at the pyrite dissolution front [103]. They also recorded pH increasing from 7 (the initial NaCl brine) to 8-10 after the reactions. In another two experiments where the pH was fixed at initial conditions (150 °C and 8 bar H_2 pressure), they found no measurable amount of sulfide at pH of 5, whereas a higher initial rate of the reduction from pyrite to pyrrhotite than in calcite buffered solution was observed at pH of 10. In their later works, they extended the studies by focusing on the effect of temperature, pressure and pH on the reduction from pyrite to pyrrhotite [105]. They found that at low temperature (<150 °C) and hydrogen partial pressure (6 bar) condition, the rate of reduction is mainly controlled by the pyrite solubility. While at higher temperature and pressure condition, the reduction is driven by the pyrrhotite precipitation. Overall, pyrite tends to be completely reduced by hydrogen to pyrrhotite within in a short time interval at temperature greater than 90 °C and hydrogen partial pressure greater than 10 bar. Besides, a higher pH (alkaline) environment would facilitate pyrrhotite precipitation even at low temperature and $\text{P}(\text{H}_2)$ conditions (Figure 2).

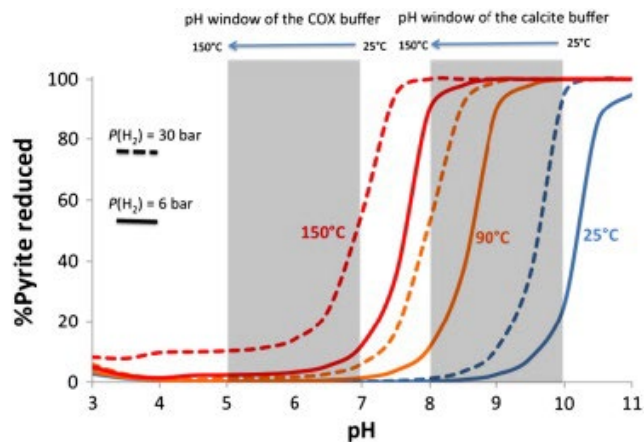


Figure 2 Percentage of pyrite dissolved as a function of pH, from 25 to 150 °C and at two different hydrogen partial pressure: 6 (solid line) and 30 bar (dotted line). The pH windows for a solution buffered by pure calcite or Cox claystone in a batch system, and in the 90–150 °C temperature range are underlined in light grey (from Truche et al. [105]).

Similar experimental results on the reduction of pyrite to pyrrhotite by hydrogen are also reported by Wiltowski et al. [106], Lambert et al. [107], Didier et al. [108] and Moslemi et al. [109]. The dissolution of pyrite in caprock may lead to integrity issues as pyrite is usually in the form of framboidal cementation within host rock. On the other hand, carbonate minerals such as calcite and dolomite commonly exist in the caprock and their reductive dissolution can increase the *in-situ* pH [59, 91]. As pointed out by Truche et al. [105], the alkaline condition can promote pyrite reduction, which may further compromise caprock integrity and generate H₂S gas. Therefore, to minimize the pyrite reduction and hydrogen conversion to H₂S, a neutral or acidic reservoirs may be more suitable.

3.1.1.4 Fe³⁺-bearing oxides

The ferric iron-bearing minerals such as goethite [FeO(OH)] and hematite (Fe₂O₃) can react with stored hydrogen through the redox reaction, where Fe³⁺ would be reduced to ferrous iron (Fe²⁺). Taking hematite for example, the oxide reduction process takes place in three steps: Fe₂O₃→Fe₃O₄→FeO→Fe [110]. However, current evidence implies that the reduction of Fe³⁺-bearing oxides can only occur in the high temperature conditions (300 to 700°C) [111-115], which are much beyond the normal geological storage conditions. However, most of the experimental works only use the pure iron oxide crystal or powder at dry condition. More detailed research needs to be conducted to evaluate the reduction of ferric iron-bearing minerals in the presence of saline brine at more complex mineralogy system (coupled with other minerals) to better characterize the fundamentals of ferric iron reduction during underground hydrogen storage from abiotic geochemical perspective.

3.1.2 Wettability and contact angle

The wettability of H₂-brine-rock system is of vital importance to assess the residual and structural storage capacity and caprock sealing ability, and also partially determines the injectivity and withdrawal rate during hydrogen cycling in subsurface porous media [116-118]. Compared to the wide studies on wettability of CO₂-brine-rock system during CO₂ geosequestration [119-123], current research on H₂ wettability during UHS is still very limited. For sandstones, Iglauer et al. [116] measured the contact angle (both advancing and receding angles) of 10% NaCl brine in the presence of hydrogen at pressures between 0.1 to 25 MPa and temperatures between 296 to 343 K. The results show that the contact angle increases with increasing temperature and pressure.

However, at the normal range of temperature and pressure at realistic subsurface storage conditions, the hydrogen wettability of sandstone shows weakly water-wet to intermediate-wet. Similar results were reported by Higgs et al. [124], Ali et al. [28] and Yekta et al. [125].

In terms of carbonate, Hosseini et al. [126] examined the hydrogen wettability of calcite with consideration of different pressure (0.1 to 20 MPa), temperature (298 to 353 K), salinity (0 to 4.95 mol/kg of NaCl + KCl), tilting plane angle (0 to 45 °) and surface roughness (root mean square, RMS = 341, 466 and 588 nm). They observed that the contact angle of brine in the presence of hydrogen on calcite surface increased with increasing of pressure, salinity and tilting plane angle, but decreases with increasing of temperature and surface roughness. Overall, similar to hydrogen wettability of quartz, the hydrogen wettability of calcite presents weakly water-wet to intermediate-wet regardless temperature and pressure. To understand the physics behind the experimental findings, Zeng et al. [127] calculated calcite surface species concentrations and surface potential in the presence of hydrogen at variety of temperature, pressure and salinity through geochemical surface complexation modelling, and the disjoining pressure on calcite surface. The results indicate that the disjoining pressure would shift to more positive with increasing temperature and decreasing salinity, intensifying the repulsion force of H₂ against calcite and thus decreasing H₂ wettability, which is consistent with experimental observations.

Since the shale caprock is usually rich in clay minerals, understanding the hydrogen wettability of clays are also very important. Ahmed et al. [33] measured the contact angles for H₂-brine-clay (kaolinite, illite, and montmorillonite) at moderate temperature of 333 K and different pressures (5 to 20 MPa) conditions. They reported that increasing pressure increases the contact angle from 13.4 to 26 ° for kaolinite, 16.3 to 31.7 ° for illite, and 19.8 to 38.6 ° for montmorillonite. While all tested clays present water-wet, kaolinite is most water-wet followed by illite and montmorillonite. The different octahedral clay sheet ('TO' and 'TOT') was claimed to account for the varying water-wetting characters [33].

A more comprehensive study was later performed by Esfandiyari et al. [128], where the contact angles of saline brines in the presence of hydrogen on the surface of calcite, dolomite, quartz, shale, anhydrite, gypsum, granite and basalt crystals were measured at various temperatures (20 to 80 °C) and pressures (10 to 100 bar). Their results confirmed that hydrogen wettability would increase with increasing pressure for not only quartz and calcite, but also for the rest of minerals. However, the contact angles are more sensitive for calcite (35 to 93 °C), dolomite (33 to 80 °C) and shale (20 to 81 °C) at different P/T, which change from strong water-wet to intermediate-wet, than gypsum (45 to 71 °C), quartz (34 to 73 °C) and basalt (17 to 35 °C), which only change from strong water-wet to weakly water-wet. Besides, hydrogen wettability was also examined on surface of mica [129, 130]. In summary, in the realistic reservoirs'

conditions, the wettability of almost every mineral within caprock is water-wet. This is in favour of caprock sealing for store hydrogen, since it provides caprock with stronger structure and residual trapping capacity to prevent hydrogen from migrating upward and de-risks the hydrogen leakage problems [126].

3.1.3 Capillary pressure and interfacial tension

Capillary pressure of hydrogen-water system in geological storage conditions are important to characterize the hydrogen migration and the capillary sealing capacity of caprock during UHS. To the best of our knowledge, hitherto, the only experimental data of capillary pressure of hydrogen-water-rock system come from Yekta et al. [125], who measured capillary pressure as function of water saturation using Triassic sandstone at “shallower” (55 bar, 20 °C) and “deeper” (100 bar, 45 °C) conditions. They found that capillary pressure increases approximately from 65 to 110 kPa with decreasing water saturation from 15 to 11%. However, changing temperature and pressure had very limited effect on capillary pressure for H₂-water system, which is different to CO₂-water system where capillary numbers strongly depend on testing temperature and pressure [131, 132]. This result suggests that capillary pressure is almost constant for the entire range of tested pressure and temperature conditions appropriate for UHS. However, a wider range of P/T conditions, more complex compositions and concentrations of formation brines, and other types of minerals particularly carbonates and clays need to be considered for the future tests.

Besides capillary pressure, interfacial tension between hydrogen and *in-situ* brine is another significant parameter that affects fluids flow and displacement within host rock and caprock, thus the entire sealing ability and containment security. Hosseini et al. [133] measured the interfacial tension between H₂ and 0.864 NaCl + 0.136 KCl solution at various temperatures (298 to 423 K), pressures (2.76 to 34.47 MPa) and salinities (0 to 4.95 mol/kg). Overall, the interfacial tension varies approximately from 45 to 80 mN/m. It decreases with increasing pressure and temperature but decreasing salinity. Similar results were reported by Chow et al. [134], Pan et al. [135], Ali et al. [129], Higgs et al. [124] and Yekeen et al. [136]. In summary, the capillary pressure and interfacial tension combined with contact angle of H₂-brine-rock system determine the wettability and capillary sealing capacity of caprock. In the realistic geological conditions for UHS, the wettability of minerals in the presence of brine and hydrogen always presents water-wet (from strong to weak water-wet dependant on P/T). The more water-wetting promotes the residual and structural trapping efficiency of caprock and reservoir rock [136]. The stronger structural trapping also decreases the height of hydrogen plume, which further decreases the buoyancy force and the pressure acting on caprock [63]. At such condition, the buoyancy force is less than the capillary force of caprock, and thus de-risks the concerns on hydrogen upward migration and overall sealing failure during UHS.

3.2 Reservoirs

3.2.1 Mineral dissolution and precipitation

The integrity of host rock in subsurface depleted gas reservoirs during UHS determines the formation petrophysical properties, including porosity, permeability, connectivity, etc., and thus the hydrogen injectivity and reproduction recovery or the entire cycling efficiency. Similar to caprock, the integrity reservoir rocks rely on the interactions of H₂-brine-mineral at *in-situ* temperature and pressure. Among all compositional minerals, the sensitive minerals defined in the section 3.1 such as carbonates (calcite, dawsonite, dolomite, magnesite and siderite), sulfates (anglesite, anhydrite, gypsum, barite and celestite), sulfide (particularly pyrite and Fe³⁺-coupled minerals (goethite and hematite and some clays containing Fe³⁺) play the critical roles since they can react with stored hydrogen and lead to reductive dissolution. The reductive dissolution of these sensitive minerals strongly affect the formation stability and integrity and thus the long-term storage capacity. For sandstone reservoirs where quartz is the mainly component and geochemically stable [35], the sensitive minerals such as calcite, siderite and anhydrite contribute as cementation. Therefore, the dissolution of these minerals can increase porosity and affect fluids flow in subsurface porous media [99]. For carbonate reservoirs where calcite and/or dolomite are the dominant minerals, the carbonates dissolution caused by the redox reactions would not only compromise the stability of matrix of porous media, but also could trigger considerable volumes of stored hydrogen [91].

Apart from the reductive dissolution, some other minerals such as illite and kaolinite can also dissolve during UHS process. However, the dissolution of these minerals is not induced by the redox reactions since there are no redox-trigger ions or RTI (Fe(3), S(6) as SO₄²⁻, C(4) as CO₃²⁻/HCO₃⁻) bonded within minerals. Their dissolutions are mainly caused by the geochemistry change as the result of reductive dissolution of sensitive minerals. Therefore, it is reasonable to classify those sorts of dissolution as secondary dissolution. For example, the redox reactions of calcite in the presence of hydrogen and brine can increase pH [59, 91] (see detailed discussion in section 3.2.2). The pH increase could accelerate the dissolution of kaolinite and illite as they tend to dissolve quickly at more alkaline conditions [137, 138]. Consequently, extra attentions are required to pay when potential depleted gas reservoirs contain high percentage of kaolinite and illite accompany by sensitive minerals to assess the geochemical integrity of target formation for underground hydrogen storage.

For subsurface hydrogen storage in porous media, depleted sandstone reservoirs are widely recognized as the premium candidate due to the high geochemical stability. From experiment point of view, Hassanpouryouzband et al. [35] systematically conducted more than 250 batch reactions using different types of sandstones (weight percentages of quartz are all greater than 80% with small fractions of carbonates, clays and other minor minerals) under various temperatures (332.15 to 353.15 K), pressures (1 to 20 MPa) and time scales (2 to 8 weeks). To quantify the mineral dissolution in the presence H₂, they tested

the compositions of fluid saturated within sandstone sample in the presence of hydrogen. To ensure that any observed geochemical reactions (if they did occur) were induced by hydrogen, a series of twin tests were performed under the same conditions where hydrogen was replaced by nitrogen. They observed a negligible difference of brine compositions before and after aging with hydrogen compared to nitrogen for all experiments, suggesting that no abiotic geochemical reactions occur for the tested sandstones, and concluded that UHS in sandstone reservoirs should be safe from geochemical perspective. Similar results were reported by Flesch et al. [99], who compared the variation of petrographic and petrophysical properties of twenty-one sandstones exposed to hydrogen under different temperatures (40 to 130 °C), pressures (10 to 20 MPa) and brine salinity (35,000 to 350,000 mg/L) in a time frame up to six weeks. They confirmed the results from Hassanpouryouzband et al. that no geochemical reactions occur for the Tertiary sandstone samples with hydrogen where pore filling cements were absent. However, for Permian and Triassic sandstones where the open and connected pores were widely filled with carbonate and anhydrite cements, these sensitive minerals were partially dissolved typically at higher salinity (because of the stronger hydrogen solubility [139]). The results were also supported by the observations that the helium porosity and nitrogen permeability increasing after hydrogen exposure, as well as the greater specific surface areas, suggesting that geochemical reactions indeed occurred with the presence of sensitive minerals as cement or infill materials.

To further understand the impact of storing hydrogen in sandstone reservoirs and upscale the experimental testing on core-size samples to reservoir size, Bo et al. [19] performed geochemical modelling to characterize the degree of mineral dissolution and hydrogen loss due to geochemical reactions during UHS in a time frame up to 30 years. The simulation input parameters, including mineralogy, reservoir temperature, pressure, porosity, water saturation and rock density, were set to match the realistic data from Mondarra and Tubridgi in Western Australia, which are the two commercial gas storage facilities that currently be operating to store natural gas and seek potential of UHS. The results show that hydrogen loss due to geochemical reactions in Mondarra (with 3 wt% of calcite) by the end of thirty years is less than 3 %, whereas only 0.75 % hydrogen loss in Tubridgi which does not contains any carbonate mineral. Overall, the abiotic geochemical reactions induced hydrogen loss is negligible, which is consistent with experimental results reported by Hassanpouryouzband et al. [35]. Besides, calcite is the only reactive mineral for the given mineral compositions applied to the modelling, and likely play the role as cement, which is also in line with observations from Flesch et al. [99]. Similar results of geochemical modelling on UHS in sandstone reservoirs was also obtained by Hemme and Van Berk [81].

In terms of carbonate reservoirs, Zeng et al. [91] performed kinetic batch simulation on Majiagou carbonate reservoir in China, which contains more than 90 wt% of calcite and dolomite. The results indicate that hydrogen loss due to geochemical reactions with carbonate mineral is 6.6% for the first year, but could

increase to 81 % after 500 years (the typical time frame of UHS ranges from weeks to several months. However, not 100 % of injected hydrogen can be withdrawn and a fraction of them would just remain underground. Therefore, it is worth to interpret the long-term impact of the interaction between trapped hydrogen with minerals [91]). The mole fraction of calcite dissolution is only 0.065%. Considering calcite is the dominate mineral with more than 90%, the 'minor' dissolution could still trigger formation integrity problem. Besides, the researcher observed a considerable amount of methane generation, which is converted from CO_3^{2-} and HCO_3^- through the redox reactions induced by hydrogen. Overall, the modelling results suggest that carbonate reservoirs are not suitable for UHS due to the several hydrogen conversion and carbonates reductive dissolution. Hassannayebi et al. [59] also conducted geochemical modelling combined thermodynamics with kinetic batch reactions in Molasse Basin of Austria to understand the fluid-rock interaction during UHS, although the percentage of carbonates are only 29 vol% with accompanying by 47 vol% of muscovite and clays (mainly illite and smectite), 20 vol% of quartz and small amounts of siderite and pyrite. Their results indicate that carbonate minerals are highly reactive to hydrogen, suggesting the potential risks of formation integrity when storing hydrogen in carbonate reservoirs, and the results are in consistence with the observations found by Zeng et al. [91].

To summarize, sandstone reservoirs are probably the best option for large-scale underground hydrogen storage in porous media due to the geochemical stability and negligible hydrogen loss. However, the presence of sensitive minerals such as calcite, anhydrite and siderite as cements in sandstone reservoirs could affect the formation porosity, permeability and connectivity, and thus the fluids flow behavior and formation integrity. However, a detailed experimental investigation on reservoir core samples to examine the petrographic and petrophysical properties in the presence of hydrogen is necessary for individual UHS project on specific site. On the other hand, carbonate reservoirs are not suitable for UHS because of the severe hydrogen conversion (either to methane or hydrogen sulfide via redox) and carbonates reductive dissolution, bringing concerns on reservoir integrity.

3.2.2 Surrounding water geochemistry

3.2.2.1 pH

pH is an important geochemical parameter that affects mineral dissolution. Unlike CO_2 geosequestration where injecting CO_2 to subsurface dramatically decreases pH to the range between 2 to 5 [140-142], for UHS, injecting H_2 to depleted gas reservoirs with presence of sensitive minerals can increase pH to the range between 9 and 12 (see Figure 3) [19, 59, 81, 91, 127, 143]. The pH increase when hydrogen involved is mainly induced by the reductive dissolution with carbonates where extra OH^- can be generated (see reductive dissolution in Table 3) [91, 143]. The pH increase would gradually constrain calcite dissolution at more alkaline condition, and that is the main reason why the rate of calcite dissolution drops at high alkaline conditions as reported by Bo et al.

[19] and Zeng et al. [91]. However, a more alkaline environment can also promote the redox reaction from pyrite (FeS_2) to pyrrhotite (FeS) [59, 107, 144], and the secondary dissolution of some clays such as kaolinite and illite (without Fe^{3+}) [137, 138], which may further impair reservoir integrity and stability.

Since the pH increase during UHS mainly contributes to the interactions between sensitive minerals and stored hydrogen, it could be expected that for sandstone reservoirs with less fractions of sensitive minerals as cement or infill materials, pH probably would not increase too much (7 to 9 [19, 143]). However, for carbonate reservoirs rich in calcite or/dolomite, we could see a bigger jump of pH and bring potential risk of storage integrity [91]. Therefore, sandstone reservoirs with limited amounts of sensitive mineral are most suitable for the large-scale UHS to de-risk the impact of pH variation on storage integrity.

3.2.2.2 *pE*

pE is defined by the negative logarithm of electron concentration in a solution and it is directly proportional to the redox potential [145]. Zeng et al. [91] simulated the *pE* variation in a long subsurface storage time in a carbonate reservoir. They observed that *pE* can dramatically drop to -10.8 after 5 years (the *pE* of surface water is around 4) and eventually reach as low as -12. Similar to pH increasing during UHS, the decrease of *pE* is also caused by the redox reaction with carbonate minerals. The strong negative *pE* shows a strong reductive environment, where the CO_3^{2-} , HCO_3^- , SO_4^{2-} and Fe^{3+} from either minerals or aqueous ions would be reduced to CH_4 , H_2S (HS^- and S^{2-}) and Fe^{2+} , respectively. Similar result was reported by Jacquemet [143], who observed that *pE* in sandstone rock after reaction with hydrogen decreased to -11.3. It is worth noting that a more negative *pE* does not mean that the solution really contains extremely high level of electrons. In fact, the solution should keep electrically neutral all the time. *pE* is actually a measurement of the potential of environment to reduce oxidant [146]. A more negative *pe* represents a greater reduction potential, indicating that the chemical species will have a tendency to gain electrons and reduce to low valence state in the presence of stored hydrogen. More detailed experimental measurements and simulations on *pE* are recommended to conduct to assess the degree of reduction potential in sandstone reservoirs to characterize the reductive dissolution of critical minerals thus the storage integrity.

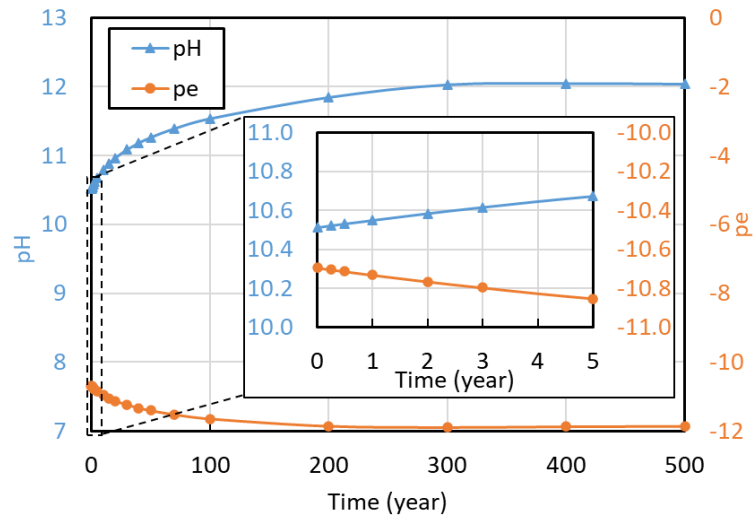


Figure 3 The variation of pH and pE over 500 years during UHS in Majiagou carbonate reservoir (from [91])

3.2.2.3 Ion composition and concentration

The change of ion composition and concentration before and after rock treated by saline brine and hydrogen can reflect the extent of geochemical reaction, and thus help assess the storage integrity issue during UHS. Hitherto, the only experimental data of ion composition and concentration regarding the subsurface hydrogen storage in porous media come from Hassanpouryouzband et al. [35], who measured the concentration of Ca, K, Mg, Ba, Fe, S, Mn and Ni before and after the sandstones saturating with brine and either hydrogen or nitrogen (which is geochemical inert gas) under realistic reservoir conditions in over 250 batch reaction experiments. With consideration the experimental measurement errors, they observed negligible differences in water compositions for the sandstones treated by hydrogen compared to nitrogen, indicating the absence of abiotic geochemical reactions for the tested sandstones within the experimental time scale (up to eight weeks). This is good for storing hydrogen in sandstone reservoirs, since negligible water chemistry change indirectly represent the negligible dissolution or precipitation of minerals, which is in favor of maintaining the reservoir integrity. Meanwhile, a stable brine chemistry would keep a constant hydrogen solubility (a higher brine concentration can lead to up to 10% more of hydrogen dissolution [19, 139]). Therefore, it is

expected to further de-risk and simplified the multi-phase flow behaviors during UHS in sandstone reservoirs (without considering other controlling factors such as hydrogen conversion to $\text{CH}_4/\text{H}_2\text{S}$, injection and reproduction rate, stress regime change, etc).

3.3 Wellbore

3.3.1 Near wellbore area

Similar to caprock and reservoir host rock, if near wellbore area at subsurface contains sensitive minerals such as carbonates, sulfates, sulfide and Fe^{3+} oxides that can trigger reductive dissolutions, and other pH-sensitive minerals such as kaolinite and illite where the dissolution would be accelerated at alkaline conditions, the stability and integrity of formation near wellbore area would be compromised. The instability of formation near wellbore could cause the failure of downhole wellbore, increasing the potential risk of fluid migration (uncontrolled release of formation fluids to surface), longevity and hydrogen cycling efficiency [147, 148]. Therefore, characterizing the *in-situ* mineralogy at near-wellbore area, limiting the fraction of sensitive minerals and a good well completion would strengthen the stability of near-wellbore area thus the wellbore integrity.

3.3.2 Cement degradation

Well cement is another important component must be considered when assessing the wellbore integrity. Subsurface cement would face the challenge of degradation from both mechanical and chemical perspective [147, 149]. The mechanical degradation is derived from the exposure to severe loading conditions, including the variation of pressure and gas volume, and thermal expansion during the hydrogen cycling [147]. The impact of chemical degradation depends on the chemical reactions such as corrosion, leaching and strength reduction of cement compounds. In general, the Portland cement clinker consists of four basic mineralogical compounds, namely alite or hatrurite ($3\text{CaO} \cdot \text{SiO}_2$), belite or larnite ($2\text{CaO} \cdot \text{SiO}_2$), celite or aluminate ($3\text{CaO} \cdot \text{Al}_2\text{O}_3$) and brownmillerite or ferrite ($4\text{CaO} \cdot \text{Al}_2\text{O}_3 \cdot \text{Fe}_2\text{O}_3$), with slight amounts of anhydrite and other component [150, 151]. By adjusting the percentage of each component, Portland cement usually contains five different classes, namely Class A, B, C, D/E and G/H, where Class G/H is most commonly used in the industry. Therefore, understanding how hydrogen reacts with cement accompanied by *in-situ* water (controlled by water-cement ratio [152]) is essential to assess the cement degradation during UHS project.

Current study on cement degradation with hydrogen involved is still scarce. Hussain et al. [153] tested the cement compressive strength and checked hydrogen bubbles within the cement by CT scanning after exposed to hydrogen and water at 120 °F and 1500 psi up to seven days using Class H cement. The

results show that the compressive strength of cement decreases with increasing ageing time to hydrogen, implying that a certain redox-sensitive minerals (particularly hematite, Fe_2O_3) experienced reductive dissolution. The generated ferrous iron (Fe^{2+}) then combined with sulphides and led to mackinawite (FeS) precipitation. This result is further supported by CT scans, which show that the numbers of trapped hydrogen bubbles inside the cement increases with increasing hydrogen saturation duration, thus promotes hematite dissolution and reduces cement's strength. From modelling point of view, Jacquemet et al. [154] simulated the geochemical reactions of Class G cement involving hydrogen at equilibrium state. Their results are in consistent with observations of Hussain et al., where hematite and ettringite [$\text{Ca}_6\text{Al}_2(\text{SO}_4)_3(\text{OH})_{12}\cdot 26\text{H}_2\text{O}$] experience reductive dissolution and form mackinawite and magnetite (Fe_3O_4). To summarize, it seems like the cement degradation due to geochemical reactions with hydrogen can only occur within sensitive minerals as the parts of cement components. While the percentage of these redox-sensitive minerals to the entire cement is minor, the hydrogen-induced reductive dissolution can still impair the cement's strength, and compromise the long-term wellbore integrity. One approach to alleviate the hydrogen-involved cement degradation is to reduce the water content. Given Class G and H types of cement with similar compositions are the most commonly used cement in the industry, and the fact that the water-cement ratio of Class H (38%) is lower than Class G (44%) [147], cycling hydrogen through the well with Class H cement is recommended than other classes of cement, although more comprehensive rock mechanics and rheological tests on Class H cement at longer time period at reservoir T/P conditions is necessary in lab-scale before conducting field trial.

4. Microbial activities

Microbial activities have been widely identified as one of the main concerns for a successful implementation of underground hydrogen storage project [5, 36, 61, 62, 89, 155-157]. Assessing the long-term effect of microbial activities on large-scale UHS in depleted gas reservoirs is typically essential, since the pre-existing carbon dioxide, sulfate and ferric ions in the reservoirs can be reduced to CH_4 , CH_3COOH , sulfite and ferrous ions by various of major microorganisms' processes, including methanogenesis, acetogenesis, sulfate reduction and iron reduction [36, 155]. Other secondary hydrogen-consuming processes may also occur such as denitrification, sulfur reduction and aerobic hydrogen oxidation [155]. The direct influence of microbial activities during UHS is to cause the hydrogen loss and contamination, where stored hydrogen is converted to CH_4 and H_2S and changes the gas mixture. The hydrogen consumption induced by the biotic processes compromises the main purpose of UHS, which aims to store hydrogen in a stable, safe and economical manner. Experience from industry on the ongoing hydrogen storage projects show that the percentage of hydrogen consumption ranges from 3% for the Underground

Sun.Storage project in Austria (converted to CH₄ through methanogenesis [158]), to 45-60% for an underground town-gas reservoir near Lobodice, Czech Republic [155, 159, 160]. The evidence of microbial activities were also reported by other projects in France [161], Germany [162] and Argentina [163]. While hydrogen conversion and contamination caused by the microbial activities can significantly affect the hydrogen cycling efficiency and increase the cost of processing of reproduced gas, it is beyond the main scope of this work (the storage integrity). In the following subsections, we will discuss the effect of microbial activities on hydrogen storage integrity during UHS in depleted gas reservoirs from three aspects: biotic mineral dissolution and precipitation, steel corrosion and core plugging or clogging, and the controlling factors that could affect the activities of different communities of bacteria, which may help screening the risk of microbial activities on storage integrity during UHS operations.

4.1 Biotic mineral dissolution and precipitation

The microbial activities induced mineral dissolutions can be classified into two categories: non-reductive dissolution and reductive dissolution. The non-reductive dissolution is caused by the acid-producing microbes, acetogens and/or heterotrophic microbes, in which the bacteria activity can generate extra H⁺ and decrease pH, thus promotes the dissolution of carbonate minerals such as calcite, dolomite, dawsonite, magnesite and siderite [155, 164]. This process generates extra CO₂ and increases the concentration of aqueous HCO₃⁻/CO₃²⁻ in saline brines, which can be further used by certain communities of microbes as source of carbon to intensify the growth and activities of bacteria by increasing cell numbers [155, 165, 166].

For the reductive dissolution, similar to the abiotic geochemical reactions, microbes can trigger the reduction of the CO₃²⁻ from carbonates to CH₄ (methanogenesis) or CH₃COOH (acetogenesis), SO₄²⁻ from sulfates and S₂²⁻ from pyrite (sulfide) to H₂S (and aqueous H₂S and HS⁻, sulfur reduction), and Fe³⁺ from ferric iron coupled oxides to Fe²⁺-coupled minerals (e.g., pyrrhotite or mackinawite with the formula of FeS, iron reduction) [36, 62, 167]. However, the presence of microbes can accelerate the reductive dissolution by providing extra electrons [5, 81]. The reductive dissolution combined with the non-reductive dissolution of these minerals as either small fractions of cementation in sandstone reservoirs or higher fractions of compositional minerals in caprock can affect the *in-situ* petrophysical properties, such as increasing porosity and permeability [99], and weaken the rock by decreasing the compressive strength [153] thus impair the storage integrity.

4.2 Core plugging/clogging

The activities of subsurface bacteria in the presence of hydrogen can lead to the plugging or clogging of pores or throats of reservoirs rocks [155]. The microbial activities induced core plugging would decrease the formation permeability and connectivity, thus reduce the injectivity and the subsequent hydrogen cycling efficiency. In general, microbial-induced plugging can be classified into two main categories: biomass plugging and mineral plugging. Biomass plugging is caused by a rapid growth and proliferation of microbial cells and associated biofilm structures in porous media [168]. The biomass plugging more likely occurs in the near-wellbore area, since the nutrient sourcing from surface through the hydrogen injection and the cells' number are the highest.

The mineral plugging is triggered by the precipitation of new mineral caused by the biotic redox reaction. For example, the ferric iron as either free aqueous ions in the saline brine or existing in the minerals (e.g., goethite and hematite) can be reduced to ferrous iron by the iron-reducing bacteria (IRB) and form new mineral phase such as pyrrhotite or mackinawite. Besides, as Dopffel et al. [155] suggested, when iron-oxidizing bacteria exist with dissolved ferric iron and oxygen, the Fe^{3+} ions can be oxidized to oxides such as ferrihydrite, goethite, magnetite. Moreover, a certain of bacteria metabolisms can lead to carbonate precipitation [169, 170]. When the surrounding source of carbon is abundant, some types of microbes can transform CO_2 to carbonate mineral combined with nitrate and sulfate reduction. However, most of previous studies on the precipitation of iron-oxides and carbonates by microbial activities didn't consider hydrogen. Since hydrogen is such a strong reductive agent, even if the precipitation of Fe^{3+} -oxides in the presence of low concentration of dissolved oxygen or carbonate mineral could occur, the injected hydrogen during UHS would probably dissolve them again through both abiotic and biotic redox reactions and form CH_4 and Fe^{2+} . Nevertheless, the microbial activities induced mineral plugging in depleted gas reservoirs needs to be further characterized particularly in the presence of hydrogen at realistic subsurface temperature and pressure conditions.

4.3 Microbial corrosion in steel and casing

Microbial corrosion in steel and casing occurs within wellbore (and associated steel related infrastructures), and is generated by the activities of microbes typically on the steel surfaces [171]. The microbial activities at optimum conditions (temperature, pH, salinity, etc.) can form biofilms on the surface of steel. A biofilm consists of cells surrounded by a matrix of exopolymeric substances such as sugars, proteins and nucleic acids and often minerals [155]. The presence of microbial biofilms is very common for microbes' communities in subsurface. The form of biofilms protects the inner microorganism from the

outer severe physical and chemical environment. Below the biofilms, the activities of microorganism can cause the corrosion on the surface of steel and casing, impair several metallic downhole components weakening the storage integrity, and ultimately trigger wellbore failure.

Among all microbial activities that could cause steel corrosion problems, the sulfate reduction induced by sulfate-reducing bacteria (SRB) usually raises more concerns. The SRB can reduce SO_4^{2-} or sulfur to H_2S by providing extra electrons and consume hydrogen. The generate acidic H_2S would then corrode steel and metallic casing and lead to H_2S -induced stress-cracking [172]. Other microbial activities such as methanogenesis, acetogenesis and iron reduction can also contribute to the steel corrosion and compromise the containment integrity [147, 173].

4.4 Controlling factors of microbial activities

While microbial activities can compromise the storage integrity by affecting mineral dissolution and precipitation through the redox reactions via different processes such as methanogenesis, acetogenesis, sulfate reduction and iron reduction, the activities are influenced by the surrounding conditions typically temperature, pH and salinity. Thaysen et al. [174] and Heinemann et al. [36] summarized those key factors controlling the activities of different classes of microorganism (see Table 4). In general, the microbial activities are most reactive at low temperature (less than 40°C), near neutral pH (6.0-7.5) and low salinity (less than 100,000 ppm) environment. Increasing reservoir temperature (storing hydrogen in deeper formation) or brine salinity (much less microbial activities induced hydrogen loss occurs in salt caverns due to the extremely high NaCl concentration [175, 176]) can effectively subdue the microbial activities. Besides, as discussed in the section 3.2.2, the surrounding pH would increase when reservoirs contain sensitive minerals that can trigger redox reactions. Experimental and modelling data show that pH can increase to 9-12 in the presence of sensitive minerals during UHS [19, 59, 81, 91, 143, 153]. As a result, it could be expected that the impact of microbial activities on biotic mineral dissolution/precipitation and associated storage integrity issues at high alkaline conditions is limited. Therefore, from only microorganism's point of view, storing hydrogen in deeper formation with higher temperature, salinity and pH condition is in favor of restraining the activities of subsurface bacteria during UHS in depleted gas reservoirs.

Table 4 Optimum and critical ranges of temperature, pH and salinity affecting microbial activities [36, 174]. Optimum condition is where the growth of microorganism reaches peaks; critical is the maximum condition within which the growth is possible.

Microbial activity	Temperature($^\circ\text{C}$)	pH	Salinity (ppm)
--------------------	---------------------------------	----	----------------

	Optimum	Critical	Optimum	Critical	Optimum	Critical
Methanogenesis	30-40	122	6.0-7.5	4.5-9.0	<60,000	200,000
Acetogenesis	20-30	72	6.0-7.5	3.6-10.7	<40,000	300,000
Sulfate reduction	20-30	113	6.0-7.5	0.8-11.5	<100,000	240,000
Iron reduction	0-30	90	6.0-7.5	1.6-9.0	<40,000	200,000

5. Faults and Fractures

Identifying the distribution and intrinsic properties of faults and fractures across reservoirs and caprock is an essential part for UHS site selection. Faults consist zones of crushed sheared and fractured rock and usually are the geomechanically weak components [177, 178]. Since the permeability of faults and fractures are greater than the matrix, the injected hydrogen could migrate upward through the activated faults/fractures, which are induced by the change of physicochemical environment and hydrogen cycling triggered stress regime change (see section 6), causing the severe loss of stored hydrogen and leading to the potential environmental and safety concerns. Therefore, it is important to characterize the intrinsic properties of faults and fractures, such as shear strength and slip, friction coefficient, permeability and conductivity, distribution, orientation and fracture angle, mineral types on fracture surfaces, and the faults/fractures surface energy change caused by the physicochemical interactions, and subsequent subcritical crack growth. Hitherto, we still lack convincing data and analysis on the performance of faults and fractures in the presence of hydrogen. However, previous experience from conventional and unconventional hydrocarbon production, hydraulic fracturing, underground gas storage and CO₂ geosequestration may bring some insights into the assessment of aforementioned faults' intrinsic properties, and pave the road for future research particularly with hydrogen involved.

5.1 Tensile damage, shear damage and shear slip

During the injection and reproduction of each hydrogen cycling period, a higher cycling rate may aggravate reservoir heterogeneity and increase bottom hole pressure. When bottom hole pressure exceeds the designed upper pressure limit and the minimum horizontal stress, it could cause the tensile damage to reservoir and caprock, leading to the activation of existing fractures and generating tensile fractures [179, 180]. The impact from tensile damage on caprock and fractures could be much severer than shear damage at gas reservoirs with shallower burial depth [179, 181]. The development of tensile fractures can

affect both permeability and permeability anisotropy [182] and accelerate hydrogen upward migration. Therefore, an accurate evaluation of tensile strength and trap ground stress is necessary to de-risk the tensile damage within caprock and faults. The leak-off test [183, 184] and AE Kaiser effect experiment [185, 186] are the two widely applied methods to test the *in-situ* stress of reservoir and caprock.

For a depleted reservoir with greater depth aiming to store hydrogen, the risk of shear damage on caprock and shear fractures could be more serious [187, 188]. The shear damage is caused by the rock mechanical heterogeneity induced by the triaxial principle stress difference and *in-situ* stress change due to the hydrogen cycling [179, 189]. Shear damage can trigger sliding deformation along the mechanical weak plane, compromising caprock stability and aggravating hydrogen upward migration. Triaxial compression test [190, 191] on core-scale sample combined with larger-scale 3D geomechanical modelling [192, 193] are commonly used to analyse the risk of shear damage on caprock and associated shear fracture propagation.

When faults and fractures are present across the reservoir and caprock, the injection and reproduction during hydrogen cycling could initiate shear slip of primary faults and extension of secondary fractures/micro-fractures along the main shear planes [194, 195]. The principle of fault shear slip is similar to shear damage, which is mainly caused by the stress regime cyclical change. However, compared to the geomechanically-weak sedimentary beddings of caprock, fault is even mechanically weaker as there is no cohesion. Therefore, the impact of stress change would be more prominent within the existing faults and fractures. The faults and fractures' slip occurs when the shear stress on fault or fracture plane is greater than the shear strength, which is the product of friction coefficient and effective normal stress [196]. Shear slip would result in severe rock deformation and fail the reservoir storage ability by damaging the caprock sealing capacity.

5.2 Friction coefficient and internal friction angle

As above discussed, fracture and fault will slip when shear stress exceeds shear strength, which is a function of effective normal stress, friction coefficient and internal friction angle. While the effective normal stress (total stress minus pore water stress [197]) and shear stress are affected by the stress regime change induced by the hydrogen cycling, the friction coefficient and internal friction angle are more like fracture intrinsic properties that are irrelevant to stress, but can be affected by surrounding physicochemical conditions. For friction coefficient (the typical value is 0.6 but can increase to 0.85 [198, 199]), it presents a greater value with higher fraction of quartz and less fraction of clays [200]. The friction coefficient would decrease when water is added into the system, playing the role as lubrication to reduce the cohesive force of the crystal particles and adjacent fracture planes [201]. While there is no evidence of friction coefficient change caused by the physical injection of gas, the geochemical reactions between CO₂ and reactive minerals such as carbonates can still

affect the friction coefficient [202]. Meanwhile, the adsorption of CO₂ on clays and organic matter can decrease the internal friction angle, and thus reduce the shear strength (assuming other parameters are constant) and increase the risk of faults shear slip. Since hydrogen is also reactive to the sensitive minerals as discussed in the section 3.1, it could be expected to see the similar results of the effect of CO₂ on friction coefficient and internal friction angle. Nevertheless, it is necessary to conduct more experiments to confirm this assumption.

5.3 Permeability

Since faults and fractures across reservoirs and caprock are the mechanical weak components, their permeability is usually higher than the surrounding matrix. Therefore, fluids and stored hydrogen would more likely migrate upward through these flow conduits [203]. During the injection and withdrawal of hydrogen cycling, the stress regime change caused faults/fractures reactivation can further increase the permeability of the fault fracture zone, aggravating hydrogen leakage from stored reservoirs. This is typically critical for caprock shales which act the role as sealing layer with ultralow permeability from the scale of nano-darcy or 10⁻²¹ m² to milli-darcy or 10⁻¹⁵ m² [204], whereas the permeability of the fault fracture zone can rise to the range from 10⁻¹⁸ to 10⁻¹¹ m² [205-208]. Therefore, it is important to test the fault zone's permeability at different stress conditions and design a safe cycling rate/bottom hole pressure to prevent the existing faults and fractures from reactivation and propagation.

5.4 Surface mineral types

Similar to reservoirs and caprock, the sensitive minerals such as carbonates, sulfates, sulfide and Fe³⁺ oxides present on the faults/fractures surface reacting with hydrogen through the redox reactions, can cause reductive dissolution thus may extend the existing micro-fractures along the main faults/fractures planes. The subsequent change of *in-situ* geochemical properties may also lead to the secondary dissolution of other minerals such as illite and kaolinite where the kinetics of dissolution highly depends on pH [137, 138]. Besides, the adsorption and desorption of hydrogen to swelling clays such as montmorillonite and laponite can lead to swelling-induced stress changes and associated fracture mechanical behaviors [108, 209], and compromise storage integrity.

5.5 Surface energy change and subcritical crack growth

The above-discussed tensile damage, shear damage and faults/fractures reactivation are mainly caused by the stress regime change during hydrogen injection and reproduction. However, even in the underground storage period where the state of stress is relatively stable, the abiotic geochemical reactions and microbial activities can still change the *in-situ* geochemical environment such as pH and salinity, affecting rock surface species concentrations, surface

potential and surface energy, and thus leads to subcritical crack growth [210-216] (see Figure 4). Subcritical crack growth corresponds to the slow fracture propagation at stress below the threshold of dynamic rupture [217-219]. When the energy release rate G (J/m^2) at tip of a crack is greater than the rock surface energy γ_s (J/m^2), the propagation of existing crack likely occur [220]. Since the surface energy change affected by the surrounding chemical conditions are kinetically controlled, compared to the instant faults slip induced by the stress change, it is expected to take much longer time to observe the impact of subcritical crack growth on storage integrity than the short-term faults slip. However, as not 100% of injected hydrogen can be withdrawn and there would be a partial of residual hydrogen trapped underground ([63, 133]), the risk of subcritical crack growth on fracture extension cannot be omitted even after the completion of UHS project. Hitherto, there still lack of data regarding the impact of hydrogen on subcritical crack growth. However, previous experience and knowledge from Earth's crust deformation [213, 221], hydrocarbons exploitation [222-224], CO_2 geosequestration [225] and mechanical weathering and rock erosion [226-228] can help to assess the impact of subcritical crack growth within fractures and reservoirs when hydrogen is involved.

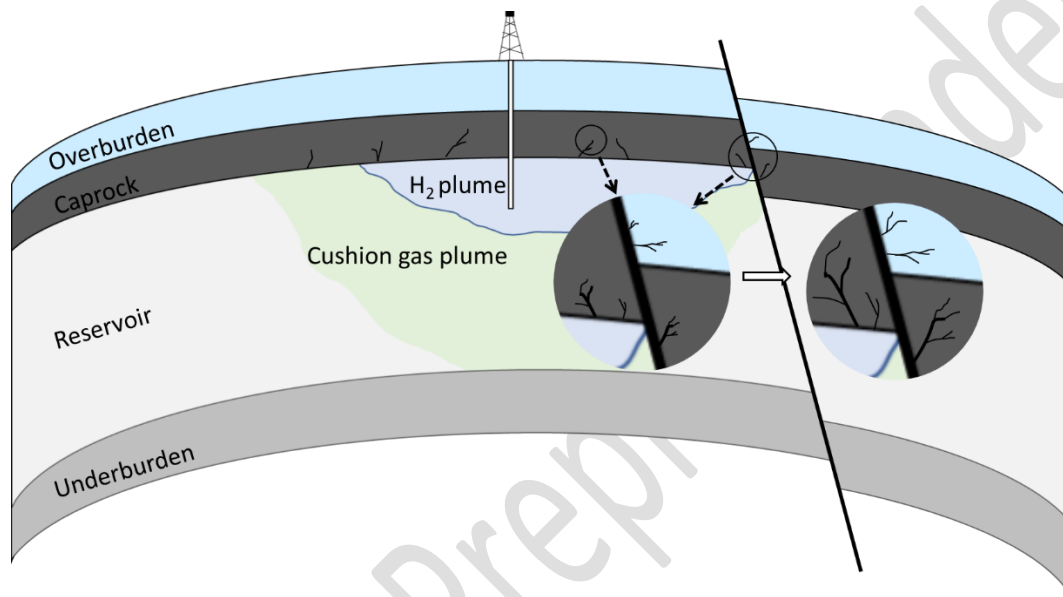


Figure 4 Schematic of microfracture propagation (subcritical crack growth) along main fractures and faults' planes due to the surface energy change.

6. Hydrogen cycling

Depending on the seasonal energy demand or the purpose of transitory storage for future domestic transportation and foreign export, the cyclic period for hydrogen injection and reproduction (withdrawal) can last from weeks to months [5]. The impact of hydrogen cycling on storage integrity mainly acts in (a) instantly changing reservoir temperature and pressure at near-wellbore area, (2) altering stress regime of reservoirs and caprock, and (3) geochemical reactions and microbial activities that affect the abiotic/biotic mineral dissolution and precipitation thus the integrity and stability. While controlling hydrogen cycling through injection rate can also change the subsurface multiphase fluid flow behavior, viscous fingering, fine migration, the mixing of store hydrogen with cushion gas, etc., they are more related to the storage performance rather than storage integrity. Therefore, the influence of hydrogen cycling on these aspects will not be discussed in this paper but are well summarized in other works [5, 16, 21, 167].

Compared to the high temperature and pressure of target storing reservoirs, the injected hydrogen has much lower temperature but higher pressure. The difference of temperature and pressure induced by hydrogen injection near wellbore area would lead to significant Joule–Thomson cooling (JTC). JTC corresponds to a temperature drop when a real gas (in our case, H_2) expands from high pressure to low pressure at constant enthalpy (i.e., adiabatic expansion) [229, 230]. The direct result of JTC is the freezing of formation brine accompanied by the generation of CO_2 or CH_4 , which reduces the injectivity and may lead to deformation at near-wellbore area [230]. Although the influence of fluctuation of temperature and pressure induced JTC on storage integrity have been widely studied for CO_2 geosequestration [231-233], there is still lack of research of the impact of JCT when hydrogen is involved, and thus calls for more efforts to assess the potential risks of JCT during UHS from both modelling and experimental perspectives.

The stress regime change caused by the cyclical hydrogen injection-withdrawal may lead to the deformation of reservoirs and caprock. For reservoirs, hydrogen cycling will periodically change the pore pressure thus the effective state of stress in the matrix, even in the area beyond the presence of hydrogen and cushion gas plume [36, 234]. This is particularly dangerous when the high rate of hydrogen injection and withdrawal is implemented, which would further lead to plastic irreversible reservoir deformation and compromise storage integrity [179, 235]. The deformation of reservoirs triggered by cyclical stress alteration may also cause reservoir compaction, decreasing formation porosity and hydrogen cycling efficiency [236-238]. For the caprock, hydrogen cycling associated stress regime change can weaken the sealing capacity by causing tensile and shear damage [177, 179, 239]. Meanwhile, the change of state of stress may generate new fractures or micro-fractures as well as activate the existing faults across caprock since they are the geologic crushed zones and geomechanically weak component [177] (also see section 5.1). Consequently, the stored hydrogen would migrate upward and cause the failure of UHS

project. However, most of the experience on deformation of reservoirs and caprock triggered by cyclic stress regime change come from underground gas storage particularly natural gas. It is still unclear how the stress alteration can affect the mechanical behavior of host rock and caprock when hydrogen participate. Nevertheless, more detailed studies need to be conducted to figure out the effect of stress regime change on reservoir and caprock deformation, fracture generation and propagation during UHS.

Furthermore, each cycle of hydrogen injection-withdrawal will change the *in-situ* fluids' compositions and phase behaviors through several physicochemical processes, including the mixing with existing trapped gas (CH₄, CO₂, etc.), adsorption and desorption typically associated with clay minerals [234, 240], dissolution and gasification from saline brine, etc. These changes combined with temperature and pressure fluctuations caused by hydrogen cycling can affect the abiotic geochemical reactions for both reductive dissolution and secondary dissolution defined in the section 3.2.1. Besides, the injection of new hydrogen from surface may introduce extra nutrient for subsurface microorganisms, thus boosting microbial activities and further accelerating biotic mineral dissolution and ultimately compromising storage integrity. Moreover, a certain portion of residual hydrogen could be trapped in the reservoirs even with the presence of cushion gas after the withdrawal process [241]. The trapped hydrogen can continue reacting with minerals and impair the long-term reservoir stability. To summarize, hitherto, we still lack enough data from both field and laboratory to assess the impact of hydrogen cycling on Joule–Thomson cooling at near-wellbore area, stress regime change induced reservoir/caprock deformation and abiotic/biotic mineral dissolution/precipitation. More laboratory and field trial tests need to perform before large-scale UHS implementation to de-risk the storage integrity issues associated within hydrogen cycling.

7. Implications, challenges and future works

To reduce the carbon emissions and alleviate global warming by holding the increase of global average temperature to well below 2 °C above pre-industrial levels [242], as an agreed deal in The 26th UN Climate Change Conference of Parties (COP26) known as Glasgow Climate Pact (GCP [243]), it is estimated that at least 113,009 Terawatt hour (TWh, [244]) should be provided by renewable energy to replace fossil fuels and to meet the global energy demand. Compared to other renewable energy such as wind, solar, tidal and wave where the generation capacity is either seasonal or affected by weather fluctuation, hydrogen is more promising as a sustainable medium for energy storing due to the nature of weather independent source and the convenience to meet seasonal balance of demand and supply [91]. To safely and economically store the tremendous volume of hydrogen, subsurface porous media is being considered as a better option than the current surface storage technology, such as high-pressure gas tanks [245, 246], cryogenic tanks [247, 248], metal hydride [249, 250], metal-organic framework [251], liquid organic hydrogen carrier [252, 253] and carbon nanotube [254, 255]. Hitherto, there are ten operating UHS projects

worldwide, where two in depleted oil and gas reservoirs, three in saline aquifers and five in salt caverns as shown in Table 1, and another 13 UHS projects are under planning [1]. The limited numbers of operating UHS sites compared to more than 680 underground gas storage projects [21] reflect the limited data and experience for successful implementation of UHS. This is typically important for storage integrity assessment, since it directly determines how far we can go to store hydrogen in subsurface in a safe manner. Therefore, it is necessary and urgent to design a screening tool to identify the potential risks from both formation petrophysical properties and implementation parameters, and associated impacts on UHS integrity.

Before going through the screening tool, it is reasonable to define the level of likelihood, consequence (or impact) and subsequent risk in the risk assessment matrix (Table 5). Likelihood is the probability that something might happen and it is often ranked on a five point scale: very likely (80%), likely (10%), possible (1%), unlikely (0.1%) and very unlikely (0.01%). Consequence is defined as the most probable result of the potential incident and it is also ranked on a five point scale: negligible, minor, moderate, severe and critical. Based on the combination of different likelihood and consequence, five levels of risk are proposed. High risk is defined to the variables or cases must be implemented cease and endorse for immediate action, since they are highly possible to fail the UHS projects. High risk (unlikely/severe, likely/moderate) is defined to the variables or cases needed to avoid or proceed with special care, since there is a small chance of cases occur but can lead to severe impact on UHS implementation. Medium high (Med Hi) is defined to the variables which are less dangerous than high-risk variables but must be reviewed to carry out improvement strategies. Medium risk is defined to the variables or cases that could impair storage integrity and may be considered for further analysis. Low/low med is defined to the variables that no further action is needed. They unlikely affect storage integrity based on the current knowledge, but could be upgraded to a higher risk level due to the change of likelihood/consequence in a specific case.

Table 5 Likelihood, consequence and risk assessment matrix. Med Hi and Low Med represent medium high and low medium risk, respectively.

Likelihood × Consequence = Risk		Consequence				
		Critical	Severe	Moderate	Minor	Negligible
Likelihood	Very likely	High	High	Med Hi	Medium	Low Med

	Likely	High	Med Hi	Medium	Low Med	Low
	Possible	Med Hi	Med Hi	Medium	Low Med	Low
	Unlikely	Med Hi	Medium	Low Med	Low Med	Low
	Very Unlikely	Medium	Medium	Low Med	Low	Low

Table 6 summarizes the controlling variables that may affect the storage integrity from geochemical reactions (section 3), microbial activities (section 4), faults and fractures (section 5) and hydrogen cycling (section 6), and assigned likelihood, consequence and risk on storage integrity, respectively. The inter connections of these variables are presented in the form of workflow shown in Figure 5. From geochemical reaction aspect, storing hydrogen in carbonate reservoirs or sandstone reservoirs/caprock with the fraction of sensitive minerals more than 10% are proposed to have medium risk, since the injected hydrogen can cause the abiotic and biotic dissolution of carbonate minerals through redox reaction discussed in the section 3.1.1 and 3.2.1, and thus compromise the formation stability and storage integrity. pH increase due to redox reaction is assigned as medium risk as high alkaline condition would accelerate the dissolution of clay minerals. Wellbore cement degradation would cause the instability of wellbore and bring the risk of collapse. However, based on a thermodynamic modelling on cement class G/H, the degree of H₂-induced cement degradation is very similar to cement hydration (reaction with brine only) compared to CH₄ and CO₂. Therefore, we rank cement degradation as medium risk but need to confirm with further rock mechanic tests. Other variables, including storing hydrogen in sandstone reservoirs with the fraction of sensitive minerals <10%, capillary leakage such as H₂ diffusion, wettability, interfacial tension and capillary pressure, and other water chemical properties are identified as low or low medium risk. For microbial activities, the four main microbial processes and bacteria accumulation induced pore plugging/clogging is in low or low medium risk in terms of storage integrity (but would be updated to medium or medium high risk when assessing H₂ conversion and contamination [36]). However, the steel/casing corrosion caused by the H₂ embrittlement in the presence of certain types of bacteria (IRB and SRB) would significantly impair the stability and longevity of wellbore. Therefore, we assign it with medium high risk which requires extra solution to minimize the propagation of crack inside the steel [147].

In terms of faults and fractures, the primary concerns come from fault shear slip, Fracture reactivation of existing fractures or propagation of new fractures, fracture orientation and fracture population/density, which are caused by the stress change during H₂ cycling. While these processes typically fault slip

unlikely happen (experience of successful operations in UGS and CCS), if they did occur, the consequence would be severe or even critical since the caprock sealing capacity would be severely compromised. For this reason, they are identified as the medium high risk. It is worth noting that the consequence of the variables in faults and fractures may change case by case. For example, different subsurface geological site has different fracture orientation, population and network density, and the magnitude of fracture reactivation/extension and fault shear slip may also be different. Therefore, a more detailed geological analysis in terms of fracture distribution in the specific depleted gas reservoir is necessary de-risk the impact of faults and fractures on storage integrity. For hydrogen cycling, the main risk is the stress magnitude change typically in the near-wellbore area, which is controlled by injection/withdrawal rate, bottom hole pressure and cycling frequency. The stress change can lead to reservoir and caprock deformation, fracture generation and propagation during UHS. While low injection/withdrawal rate is preferred to minimize the potential risk [5], a higher rate may be requested due to the energy demand in market and overall economic feasibility. Therefore, the variables in H₂ cycling are assigned with medium risk, which means they are under control but need special attention to avoid integrity failure. It is also worthwhile recalling the fact that we only focus on screening the risk of storage integrity in this paper. Some other variables such as the role of cushion gas are not discussed because they are more relevant to other UHS issues, such as hydrogen conversion and contamination, storage performance, surface facilities and wells, economic assessment, and planning, regulation, safety and society. Even the same variable may have different risk in terms of different screening perspectives. For example, the hydrogen diffusion has low medium risk on caprock sealing capacity due to the limited distance of upward migration [81]. However, it may affect the purity of stored hydrogen and reproduction efficiency through the mixing with cushion gas [79, 256], and could be upgraded to medium or medium high risk in storage performance screening tool, which is beyond the scope of this work though.

Table 6 Controlling variables, risks and impacts on storage integrity during UHS.

Variables		Caprock	Reservoir	Wellbore	Values/characteristics		Likelihood	Consequence	Risk
Geochemical reactions	Primary	N/A	Carbonate reservoirs (including near wellbore area)		Carbonate dissolution	<0.01%	Very likely	Minor	Medium
		N/A	Sandstone reservoirs (including near wellbore area)		Fraction of sensitive minerals	<5%	Likely	Negligible	Low
		Argillaceous	N/A	N/A		5 to 10%	Likely	Minor	Low Med

		shales				>10%	Likely	Moderate	Medium
	Secondary	H ₂ diffusion	N/A	N/A	14.4 to 218.9 × 10 ⁻⁸ m ² /s	Capillary leakage	Likely	Minor	Low Med
		Wettability	N/A	N/A	Strong to weak water-wet		Likely	Minor	Low Med
		Interfacial tension	N/A	N/A	45 to 80 mN/m		Likely	Minor	Low Med
		Capillary pressure	N/A	N/A	65 to 110 kPa		Likely	Minor	Low Med
		N/A	pH	N/A	7 to 12	Likely	Moderate	Medium	
		N/A	pE	N/A	4 to -12	Likely	Negligible	Low	
		N/A	Ion compositions and concentrations	N/A	Site dependant	Very unlikely	Negligible	Low	
		N/A	N/A	Cement degradation	Limited further degradation after cement hydration	Likely	Moderate	Medium	
Microbial activities		Primary	Methanogenesis			CO ₂ + 4H ₂ = CH ₄ + 2H ₂ O	Likely	Minor	Low Med
	Acetogenesis			2CO ₂ + 4H ₂ = CH ₃ COOH + 2H ₂ O	Likely	Minor	Low Med		

		Sulfate reduction			$\text{SO}_4^{2-} + 5\text{H}_2 = \text{H}_2\text{S} + 2\text{H}_2\text{O}$	Likely	Minor	Low Med
		Iron reduction			$2\text{Fe}^{3+} + \text{H}_2 = 2\text{Fe}^{2+} + 2\text{H}^+$	Likely	Minor	Low Med
	Secondary	N/A	Pore plugging/clogging	N/A	Bacteria accumulation	Unlikely	Negligible	Low
		N/A	N/A	Steel/ casing corrosion	H_2 embrittlement	Very likely	Severe	Med Hi
Faults and fractures	Primary	Fault shear slip		N/A	Stress change	Unlikely	Critical	Med Hi
		Fracture reactivation/propagation		N/A	Stress change	Possible	Severe	Med Hi
		Fracture orientation		N/A	Side dependant	Possible	Severe	Med Hi
		Fracture population/density		N/A	Side dependant	Possible	Severe	Med Hi
	Secondary	Friction coefficient		N/A	0.85	Very unlikely	Negligible	Low
		Fault permeability		N/A	10^{-18} to 10^{-11} m ²	Possible	Moderate	Medium
		Surface mineral types		N/A	Sensitive minerals	Likely	Minor	Low Med
		Subcritical crack growth		N/A	Surface energy	Possible	Minor	Low Med
Hydrogen cycling	Primary	Stress magnitude change			Rock failure	Likely	Moderate	Medium
	Secondary	Injection rate			Low rate is preferable	Likely	Moderate	Medium
		Withdrawn rate			Low rate is preferable	Likely	Moderate	Medium

	Bottom hole pressure	Site dependant	Likely	Moderate	Medium
	Cycling frequency (number and duration)	Site dependant	Likely	Minor	Low Med
	Number of legacy well	Site dependant	Possible	Moderate	Medium

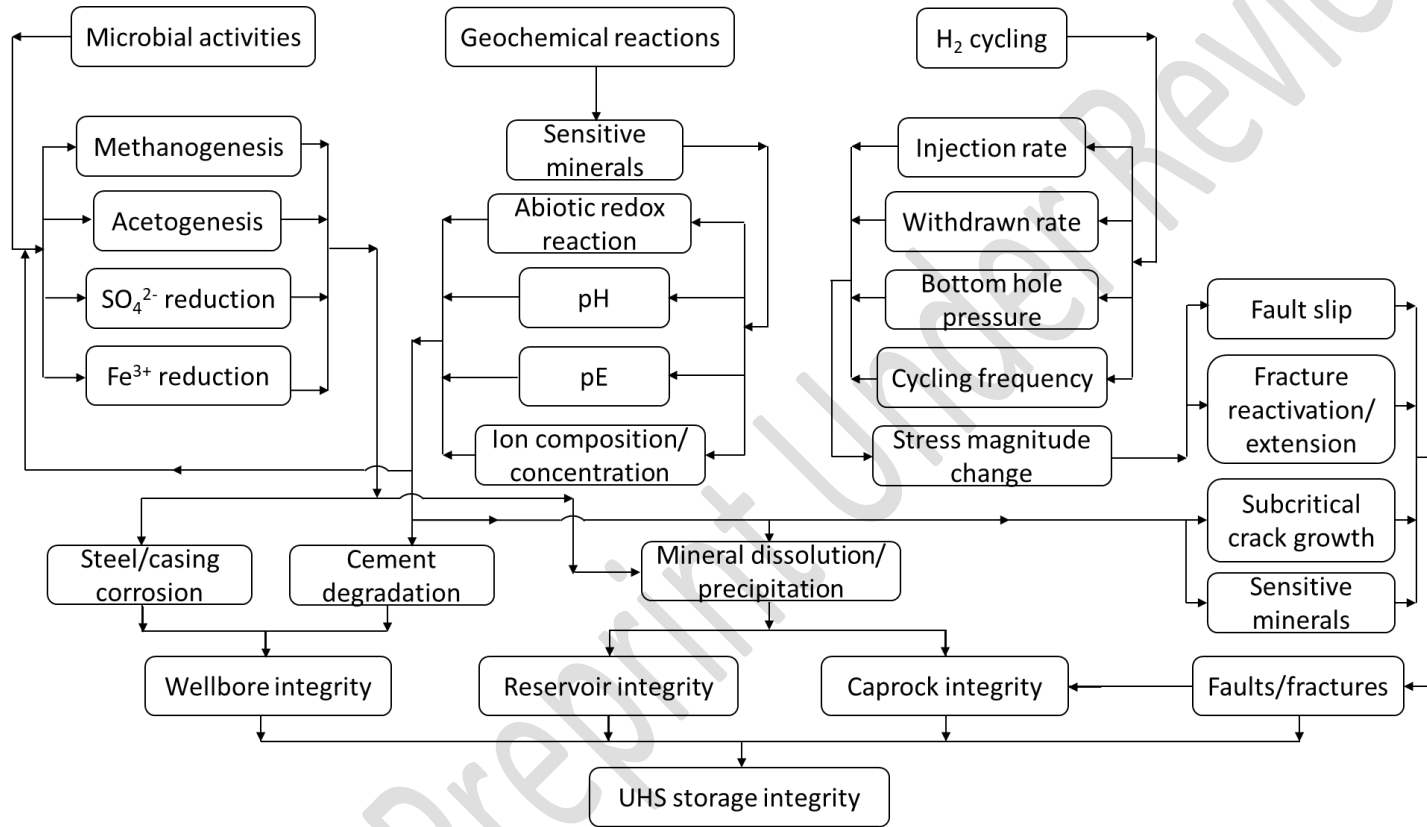


Figure 5 Workflow of interconnection of identified variables affecting storage integrity during UHS.

Sometimes, although the identified risk of certain variables is high or medium, they can be controlled with proper measures or the degree of danger would be alleviated with consideration other parameters (so called risk mitigation). In these cases, the lower occurrence of medium high or medium risk would degrade the impact on real UHS implementation. A good example is carbonate reservoirs. We do classify the medium risk of storing hydrogen in carbonate reservoirs due to the severe dissolution of carbonate minerals and associated hydrogen loss. However, since we've already known these risks, we will not inject hydrogen into depleted carbonate reservoirs or sandstone reservoirs containing high fractions of sensitive minerals. Therefore, the potential high risk regarding the mineralogy is minimized. Similarly, although the microbial activities have medium risk on critical mineral dissolution, they are only reactive in the optimum conditions, e.g., low temperature ($< 40\text{ }^{\circ}\text{C}$), neutral pH (6 to 7.5) and low salinity ($< 60,000\text{ ppm}$) conditions (section 4.4). Reservoirs with higher temperature and salinity can restrain the microbial activities. Besides, with the presence of sensitive minerals and stored hydrogen, the *in-situ* pH can increase to the range between 9 and 12 (section 3.2.2), which would further limit the impact of microbial activities on storage integrity (from this point view, a small fraction of sensitive minerals that will not affect overall rock mechanical properties after the redox reactions with hydrogen could be in favor of inhibiting microbial activities). However, the stress change related variables, including faults and fractures shear slip, reactivation and propagation, rate of injection and withdrawal, and bottom hole pressure are identified as medium high or medium. Although a low rate of injection and withdrawal is suggested to minimize the risk on stress regime alteration, lateral spreading, fingering, fluid conning, etc. [5], due to the *in-situ* heterogeneity, the injection and withdrawal even under designed threshold may still trigger unexpected issues affecting the storage integrity. In fact, experience from more than 50 years in petroleum industry tell us that most of failures during gas extraction and injection occur at wellbore or near wellbore area due to the faulty casing, cementing and inappropriate production rate and bottom hole pressure, which eventually cause the excessive fluctuation of state of stress and well integrity problems, triggering the gases and liquids leakage and failing the whole project [257]. Therefore, the stress related impacts are characterized as medium to medium high for UHS and need special care to proceed.

The aforementioned screening tool summarizes the possible variables that could affect storage integrity during underground hydrogen storage in porous media particularly in depleted gas reservoirs, and the corresponding levels of likelihood, consequence and risk. However, the identified degrees of risk and impact are based on the current knowledge from limited studies of simulations, experiments and field pilot projects. The lack of more detailed research and data, to some extent, may influence the judgement of assigned risk. Therefore, much more efforts from reservoir engineer, geochemist, geophysicist, petrophysicist, geologist, rock mechanics engineer, microbiologist, etc., from both academia and industry are calling for to assess the possibility of storing

hydrogen in subsurface and de-risk the potential integrity issues. For example, current geochemical modelling on mineral dissolution and precipitation in reservoirs and caprock, either from thermodynamic or kinetics perspective, highly relies on the database to simulate the comprehensive fluid-rock interactions [19, 59, 81, 82, 91, 143, 154]. However, the existing geochemical database needs to be updated by calibrating the equilibrium constant and reaction enthalpy in thermodynamic modelling, and the rate constant, Arrhenius activation energy and reaction order in kinetics modelling when hydrogen is involved. For microorganism, since their activities are highly dependent on the surrounding temperature and water chemistry typically pH and salinity, it is important to measure the biotic hydrogen consumption rate for each type of microbial reactions (i.e., methanogenesis, acetogenesis, sulfate reduction and Fe^{3+} reduction) at different temperature, pressure, pH, salinity and in the presence of different types of rock (e.g., sandstones, carbonates and shales, etc). In terms of rock mechanics, hitherto, there is still lack of reliable data on how hydrogen can affect rock mechanical properties such as compressive strength, Young's modulus and brittleness index, etc., and stress regime change induced tensile and shear damage, faults shear slip, fracture reactivation and propagation in reservoirs, caprock and near-wellbore area. One unique property differentiating hydrogen from other stored gas such as CO_2 , CH_4 and N_2 is that hydrogen is a strong reduction agent that can trigger the redox reaction with sensitive minerals. During redox process, the electrons would transfer from hydrogen to other ions at high valence. Meanwhile, the presence of microorganisms can provide extra electrons. However, it is still unclear how the transferred electrons would affect rock mechanical behaviors. Future works are required to address these problems to narrow the limitation fence and de-risk the challenges on storage integrity issues during underground hydrogen storage in porous media.

8. Conclusions

While underground hydrogen storage is considered as the best option to economically store hydrogen on the scale to replace fossil fuel to meet energy demand, current experience and understanding of UHS are still very limited, which impedes the industrial implementation in large-scale. Hydrogen storage integrity is one of the main concerns in UHS associated with geochemical reactions, microbial reactions and hydrogen cycling process with presence of fractures and faults. This work delineates the scientific and technological challenges and knowledge gaps, which need to be further examined, to mitigate and manage hydrogen storage integrity risks and uncertainties. In each of the primary variables, various secondary variables were discussed in detail, including the role of sensitive minerals on dissolution/precipitation, capillary leakage which consists of wettability and contact angle, capillary pressure and interfacial tension, water chemistry change (pH, pE, ion concentration and composition), cement degradation, microbial corrosion in steel and casing, different mechanisms of faults slip and fracture reactivation and propagation, etc. More importantly, a state-of-the-art technical screening tool was developed for the

first time to assess risks and uncertainties regarding storage integrity, which can help industry operators selecting best candidate for pilot tests of underground hydrogen storage in depleted gas reservoirs.

Acknowledgement

Q. Xie, M. Sarmadivaleh and A. Saeedi are thankful to Future Energy Export CRC and Beach Energy Limit for supporting this work and funding L. Zeng's postdoctoral research through the project - Enabling Large-Scale Hydrogen Underground Storage in Porous Media (21.RP2.0091). The authors also gratefully acknowledge the discussions with Chris Elders, Mauricio Di Lorenzo and Qun Lin from Curtin University, and Michael Roberts, Alexandra Bennett, Claire Dowling, Joe Collins, Jason Storey and Glen Buick from Beach Energy Ltd for the constructive comments to improve the quality of this work.

References

1. Sambo, C., et al., *A review on worldwide underground hydrogen storage operating and potential fields*. International Journal of Hydrogen Energy, 2022. **47**(54): p. 22840-22880.
2. Zou, C., et al., *Energy revolution: From a fossil energy era to a new energy era*. Natural Gas Industry B, 2016. **3**(1): p. 1-11.
3. Mahfuz, M.H., et al., *Exergetic analysis of a solar thermal power system with PCM storage*. Energy Conversion and Management, 2014. **78**: p. 486-492.
4. IEA. *Renewable electricity growth is accelerating faster than ever worldwide, supporting the emergence of the new global energy economy*. 2021 [cited 2021 December 1]; Available from: <https://www.iea.org/news/renewable-electricity-growth-is-accelerating-faster-than-ever-worldwide-supporting-the-emergence-of-the-new-global-energy-economy>.
5. Zivar, D., S. Kumar, and J. Foroozesh, *Underground hydrogen storage: A comprehensive review*. International Journal of Hydrogen Energy, 2020.
6. Engeland, K., et al., *Space-time variability of climate variables and intermittent renewable electricity production—A review*. 2017. **79**: p. 600-617.
7. Heide, D., et al., *Seasonal optimal mix of wind and solar power in a future, highly renewable Europe*. 2010. **35**(11): p. 2483-2489.
8. Heinemann, N., et al., *Enabling large-scale hydrogen storage in porous media – the scientific challenges*. Energy & Environmental Science, 2021.
9. Mouli-Castillo, J., N. Heinemann, and K. Edlmann, *Mapping geological hydrogen storage capacity and regional heating demands: An applied UK case study*. Applied Energy, 2021. **283**: p. 116348.
10. Gabrielli, P., et al., *Seasonal energy storage for zero-emissions multi-energy systems via underground hydrogen storage*. Renewable and Sustainable Energy Reviews, 2020. **121**: p. 109629.
11. Denholm, P. and T.J.R.e. Mai, *Timescales of energy storage needed for reducing renewable energy curtailment*. 2019. **130**: p. 388-399.
12. Pinel, P., et al., *A review of available methods for seasonal storage of solar thermal energy in residential applications*. 2011. **15**(7): p. 3341-3359.
13. Sordakis, K., et al., *Homogeneous catalysis for sustainable hydrogen storage in formic acid and alcohols*. 2018. **118**(2): p. 372-433.

14. Parra, D., et al., *A review on the role, cost and value of hydrogen energy systems for deep decarbonisation*. Renewable and Sustainable Energy Reviews, 2019. **101**: p. 279-294.
15. Lebrouhi, B.E., et al., *Global hydrogen development - A technological and geopolitical overview*. International Journal of Hydrogen Energy, 2022. **47**(11): p. 7016-7048.
16. Abdalla, A.M., et al., *Hydrogen production, storage, transportation and key challenges with applications: A review*. Energy Conversion and Management, 2018. **165**: p. 602-627.
17. Barthelemy, H., M. Weber, and F. Barbier, *Hydrogen storage: Recent improvements and industrial perspectives*. International Journal of Hydrogen Energy, 2017. **42**(11): p. 7254-7262.
18. Ren, J., et al., *Current research trends and perspectives on materials-based hydrogen storage solutions: A critical review*. International Journal of Hydrogen Energy, 2017. **42**(1): p. 289-311.
19. Bo, Z., et al., *Geochemical reactions-induced hydrogen loss during underground hydrogen storage in sandstone reservoirs*. International Journal of Hydrogen Energy, 2021. **46**(38): p. 19998-20009.
20. Zivar, D., S. Kumar, and J. Foroozesh, *Underground hydrogen storage: A comprehensive review*. International Journal of Hydrogen Energy, 2021. **46**(45): p. 23436-23462.
21. Tarkowski, R., *Underground hydrogen storage: Characteristics and prospects*. Renewable and Sustainable Energy Reviews, 2019. **105**: p. 86-94.
22. Lemieux, A., K. Sharp, and A. Shkarupin, *Preliminary assessment of underground hydrogen storage sites in Ontario, Canada*. International Journal of Hydrogen Energy, 2019. **44**(29): p. 15193-15204.
23. Abe, J.O., et al., *Hydrogen energy, economy and storage: Review and recommendation*. International Journal of Hydrogen Energy, 2019. **44**(29): p. 15072-15086.
24. Megía, P.J., et al., *Hydrogen Production Technologies: From Fossil Fuels toward Renewable Sources. A Mini Review*. Energy & Fuels, 2021. **35**(20): p. 16403-16415.
25. Hassanpouryouzband, A., et al., *Offshore Geological Storage of Hydrogen: Is This Our Best Option to Achieve Net-Zero?* ACS Energy Letters, 2021. **6**(6): p. 2181-2186.
26. Pan, B., et al., *Underground hydrogen storage: Influencing parameters and future outlook*. Advances in Colloid and Interface Science, 2021. **294**: p. 102473.
27. Iglauer, S., et al., *Hydrogen Adsorption on Sub-Bituminous Coal: Implications for Hydrogen Geo-Storage*. Geophysical Research Letters, 2021. **48**(10): p. e2021GL092976.
28. Ali, M., et al., *Hydrogen wettability of quartz substrates exposed to organic acids; Implications for hydrogen geo-storage in sandstone reservoirs*. Journal of Petroleum Science and Engineering, 2021. **207**: p. 109081.
29. Suckale, J., *Moderate-to-large seismicity induced by hydrocarbon production*. The Leading Edge, 2010. **29**(3): p. 310-319.
30. Segall, P., *Earthquakes triggered by fluid extraction*. Geology, 1989. **17**(10): p. 942-946.
31. Preisig, M. and J.H.J.I.J.o.G.G.C. Prévost, *Coupled multi-phase thermo-poromechanical effects. Case study: CO2 injection at In Salah, Algeria*. 2011. **5**(4): p. 1055-1064.

32. Ali, M., et al., *Influence of organic molecules on wetting characteristics of mica/H₂/brine systems: Implications for hydrogen structural trapping capacities*. Journal of Colloid and Interface Science, 2022. **608**: p. 1739-1749.
33. Al-Yaseri, A., et al., *Hydrogen wettability of clays: Implications for underground hydrogen storage*. International Journal of Hydrogen Energy, 2021. **46**(69): p. 34356-34361.
34. Tarkowski, R. and B. Uliasz-Misiak, *Towards underground hydrogen storage: A review of barriers*. Renewable and Sustainable Energy Reviews, 2022. **162**: p. 112451.
35. Hassanpouryouzband, A., et al., *Geological Hydrogen Storage: Geochemical Reactivity of Hydrogen with Sandstone Reservoirs*. ACS Energy Letters, 2022: p. 2203-2210.
36. Heinemann, N., et al., *Enabling large-scale hydrogen storage in porous media—the scientific challenges*. Energy & Environmental Science, 2021. **14**(2): p. 853-864.
37. 03/06/2021; Available from: <https://gtr.ukri.org/projects?ref=EP%2FS027815%2F1#/tabOverview>.
38. Beutel, T. and S. Black, *Salt deposits and gas cavern storage in the UK with a case study of salt exploration from Cheshire*. Oil Gas European Magazine, 2005. **1**(2005): p. 31-35.
39. 22/10/2007; Available from: <https://investors.linde.com/archive/praxair/news/2007/praxair-commercializes-industrys-only-hydrogen-storage>.
40. Laban, M., *Hydrogen Storage in Salt Caverns: Chemical modelling and analysis of large-scale hydrogen storage in underground salt caverns*. 2020.
41. Forsberg, C., *Assessment of nuclear-hydrogen synergies with renewable energy systems and coal liquefaction processes*. ORNL/TM-2006/114, August, 2006.
42. 2015; Available from: <http://hyunder.eu/>.
43. 14/06/2021; Available from: <https://www.underground-sun-storage.at/en/project/project-description.html>.
44. 04/05/2021; Available from: <https://company-announcements.afr.com/asx/adx/45a6e259-ac63-11eb-99b6-4a6c8bdc50da.pdf>.
45. 01/06/2021; Available from: https://www.euramet.org/research-innovation/search-research-projects/details/project/metrology-for-advanced-hydrogen-storage-solutions/?tx_eurametctcp_project%5Baction%5D=show&tx_eurametctcp_project%5Bcontroller%5D=Project&cHash=44fb6812cfaa610d1772e23e4ade526e.
46. 13/06/2021; Available from: <https://projecten.topsectorenergie.nl/projecten/large-scale-energy-storage-in-salt-caverns-and-depleted-gas-fields-00032959>.
47. Groenenberg, R., et al., *Large-Scale Energy Storage in Salt Caverns and Depleted Fields (LSES)—Project Findings*. 2020.
48. Plaat, H., *Underground gas storage: Why and how*. Geological Society, London, Special Publications, 2009. **313**(1): p. 25-37.
49. Evans, D.J. and R.A. Chadwick. *Underground gas storage: Worldwide experiences and future development in the UK and Europe*. 2009. Geological Society of London.
50. Zhang, J., et al., *Natural gas market and underground gas storage development in China*. Journal of Energy Storage, 2020. **29**: p. 101338.
51. Azin, R., A. Nasiri, and J. Entezari, *Underground gas storage in a partially depleted gas reservoir*. Oil & Gas Science and Technology-Revue de l'IFP, 2008. **63**(6): p. 691-703.

52. Raza, A., et al., *Significant aspects of carbon capture and storage – A review*. Petroleum, 2019. **5**(4): p. 335-340.
53. Raza, A., et al., *A screening criterion for selection of suitable CO₂ storage sites*. Journal of Natural Gas Science and Engineering, 2016. **28**: p. 317-327.
54. Boot-Handford, M.E., et al., *Carbon capture and storage update*. Energy & Environmental Science, 2014. **7**(1): p. 130-189.
55. Züttel, A., *Hydrogen storage methods*. Naturwissenschaften, 2004. **91**(4): p. 157-172.
56. Lord, A.S., *Overview of geologic storage of natural gas with an emphasis on assessing the feasibility of storing hydrogen*. SAND2009-5878, Sandia National Laboratory, Albuquerque, NM, 2009.
57. Reitenbach, V., et al., *Influence of added hydrogen on underground gas storage: a review of key issues*. Environmental Earth Sciences, 2015. **73**: p. 6927-6937.
58. Tarkowski, R., *Perspectives of using the geological subsurface for hydrogen storage in Poland*. International Journal of Hydrogen Energy, 2017. **42**(1): p. 347-355.
59. Hassannayebi, N., et al., *Underground hydrogen storage: application of geochemical modelling in a case study in the Molasse Basin, Upper Austria*. Environmental Earth Sciences, 2019. **78**(5): p. 1-14.
60. Reitenbach, V., et al., *Influence of added hydrogen on underground gas storage: a review of key issues*. Environmental Earth Sciences, 2015. **73**(11): p. 6927-6937.
61. Liebscher, A., J. Wackerl, and M. Streibel, *Geologic Storage of Hydrogen – Fundamentals, Processing, and Projects, in Hydrogen Science and Engineering : Materials, Processes, Systems and Technology*. 2016. p. 629-658.
62. Papadias, D.D. and R.K. Ahluwalia, *Bulk storage of hydrogen*. International Journal of Hydrogen Energy, 2021. **46**(70): p. 34527-34541.
63. Iglauer, S., *Optimum geological storage depths for structural H₂ geo-storage*. Journal of Petroleum Science and Engineering, 2021: p. 109498.
64. Guo, B., J. Molinard, and R. Lee. *A general solution of gas/water coning problem for horizontal wells*. in *European Petroleum Conference*. 1992. OnePetro.
65. Abass, H. and D. Bass. *The critical production rate in water-coning system*. in *Permian Basin Oil and Gas Recovery Conference*. 1988. OnePetro.
66. Rajan, V.S. and R.W. Luhning, *Water coning suppression*. Journal of Canadian Petroleum Technology, 1993. **32**(04).
67. Paterson, L., *The implications of fingering in underground hydrogen storage*. International journal of hydrogen energy, 1983. **8**(1): p. 53-59.
68. Wiesenburg, D.A. and N.L. Guinasso Jr, *Equilibrium solubilities of methane, carbon monoxide, and hydrogen in water and sea water*. Journal of chemical and engineering data, 1979. **24**(4): p. 356-360.
69. Suleimenov, O. and R. Krupp, *Solubility of hydrogen sulfide in pure water and in NaCl solutions, from 20 to 320 C and at saturation pressures*. Geochimica et Cosmochimica Acta, 1994. **58**(11): p. 2433-2444.
70. Duan, Z., et al., *The prediction of methane solubility in natural waters to high ionic strength from 0 to 250 C and from 0 to 1600 bar*. Geochimica et Cosmochimica Acta, 1992. **56**(4): p. 1451-1460.
71. Duan, Z. and R. Sun, *An improved model calculating CO₂ solubility in pure water and aqueous NaCl solutions from 273 to 533 K and from 0 to 2000 bar*. Chemical geology, 2003. **193**(3-4): p. 257-271.
72. Li, D., C. Beyer, and S. Bauer, *A unified phase equilibrium model for hydrogen solubility and solution density*. International Journal of Hydrogen Energy, 2018. **43**(1): p. 512-529.

73. Chabab, S., et al., *Measurements and predictive models of high-pressure H₂ solubility in brine (H₂O+ NaCl) for underground hydrogen storage application*. International Journal of Hydrogen Energy, 2020. **45**(56): p. 32206-32220.
74. Parkhurst, D.L. and C. Appelo, *Description of input and examples for PHREEQC version 3: a computer program for speciation, batch-reaction, one-dimensional transport, and inverse geochemical calculations*. 2013, US Geological Survey.
75. Ferrell, R. and D. Himmelblau, *Diffusion coefficients of hydrogen and helium in water*. AIChE Journal, 1967. **13**(4): p. 702-708.
76. Tamimi, A., E.B. Rinker, and O.C. Sandall, *Diffusion coefficients for hydrogen sulfide, carbon dioxide, and nitrous oxide in water over the temperature range 293-368 K*. Journal of Chemical and Engineering data, 1994. **39**(2): p. 330-332.
77. Witherspoon, P. and D. Saraf, *Diffusion of Methane, Ethane, Propane, and n-Butane in Water from 25 to 43*. The Journal of Physical Chemistry, 1965. **69**(11): p. 3752-3755.
78. Shen, L. and Z. Chen, *Critical review of the impact of tortuosity on diffusion*. Chemical Engineering Science, 2007. **62**(14): p. 3748-3755.
79. Feldmann, F., et al., *Numerical simulation of hydrodynamic and gas mixing processes in underground hydrogen storages*. Environmental Earth Sciences, 2016. **75**(16): p. 1-15.
80. Yekta, A.E., M. Pichavant, and P. Audigane, *Evaluation of geochemical reactivity of hydrogen in sandstone: Application to geological storage*. Applied Geochemistry, 2018. **95**: p. 182-194.
81. Hemme, C. and W. Van Berk, *Hydrogeochemical modeling to identify potential risks of underground hydrogen storage in depleted gas fields*. Applied Sciences, 2018. **8**(11): p. 2282.
82. Labus, K. and R. Tarkowski, *Modeling hydrogen–rock–brine interactions for the Jurassic reservoir and cap rocks from Polish Lowlands*. International Journal of Hydrogen Energy, 2022. **47**(20): p. 10947-10962.
83. Ganzer, L., et al. *The H2STORE project-experimental and numerical simulation approach to investigate processes in underground hydrogen reservoir storage*. in *EAGE annual conference & exhibition incorporating SPE Europec*. 2013. OnePetro.
84. Palandri, J.L. and Y.K. Kharaka, *A compilation of rate parameters of water-mineral interaction kinetics for application to geochemical modeling*. 2004, Geological Survey Menlo Park CA.
85. Golubev, S.V., et al., *Siderite dissolution kinetics in acidic aqueous solutions from 25 to 100 °C and 0 to 50 atm pCO₂*. Chemical Geology, 2009. **265**(1): p. 13-19.
86. Giardini, A.A. and C.A. Salotti, *Kinetics and relations in the calcite-hydrogen reaction and relations in the dolomite-hydrogen and siderite-hydrogen systems*. American Mineralogist: Journal of Earth and Planetary Materials, 1969. **54**(7-8): p. 1151-1172.
87. Harris, P.M., C.G.S.C. Kendall, and I. Lerche, *Carbonate cementation—a brief review*. 1985.
88. Morad, S., *Carbonate cementation in sandstones: distribution patterns and geochemical evolution*. 2009: John Wiley & Sons.
89. Amid, A., D. Mignard, and M. Wilkinson, *Seasonal storage of hydrogen in a depleted natural gas reservoir*. International Journal of Hydrogen Energy, 2016. **41**(12): p. 5549-5558.
90. Pichler, M. *Assesment of hydrogen rock interaction during geological storage of CH₄-H₂ mixtures*. in *Second EAGE Sustainable Earth Sciences (SES) Conference and Exhibition*. 2013. European Association of Geoscientists & Engineers.

91. Zeng, L., et al., *Hydrogen storage in Majiagou carbonate reservoir in China: Geochemical modelling on carbonate dissolution and hydrogen loss*. International Journal of Hydrogen Energy, 2022.
92. Pudlo, D., et al. *The impact of hydrogen on potential underground energy reservoirs*. in EGU General Assembly Conference Abstracts. 2018.
93. Bensing, J.P., et al., *Hydrogen-induced calcite dissolution in Amaltheenton Formation claystones: Implications for underground hydrogen storage caprock integrity*. International Journal of Hydrogen Energy, 2022.
94. Bensing, J.P., et al., *HYDROGEN-INDUCED CALCITE DISSOLUTION IN AMALTHEENTON FORMATION CLAYSTONES: IMPLICATIONS FOR UNDERGROUND HYDROGEN STORAGE CAPROCK INTEGRITY*. 2022.
95. Carroll, J.J. and A.E. Mather, *The solubility of hydrogen sulphide in water from 0 to 90 C and pressures to 1 MPa*. Geochimica et Cosmochimica Acta, 1989. **53**(6): p. 1163-1170.
96. Crotagino, F., *Large-scale hydrogen storage*, in *Storing energy*. 2022, Elsevier. p. 613-632.
97. Lassin, A., M. Dymitrowska, and M. Azaroual, *Hydrogen solubility in pore water of partially saturated argillites: Application to Callovo-Oxfordian clayrock in the context of a nuclear waste geological disposal*. Physics and Chemistry of the Earth, Parts A/B/C, 2011. **36**(17-18): p. 1721-1728.
98. Henkel, S., et al. *Effects of H₂ and CO₂ Underground Storage in Natural Pore Reservoirs-Findings by SEM and AFM Techniques*. in *The Third Sustainable Earth Sciences Conference and Exhibition*. 2015. European Association of Geoscientists & Engineers.
99. Flesch, S., et al., *Hydrogen underground storage—Petrographic and petrophysical variations in reservoir sandstones from laboratory experiments under simulated reservoir conditions*. International Journal of Hydrogen Energy, 2018. **43**(45): p. 20822-20835.
100. Truche, L., et al., *Sulphide mineral reactions in clay-rich rock induced by high hydrogen pressure. Application to disturbed or natural settings up to 250 C and 30 bar*. Chemical Geology, 2013. **351**: p. 217-228.
101. Truche, L., et al., *Experimental reduction of aqueous sulphate by hydrogen under hydrothermal conditions: implication for the nuclear waste storage*. Geochimica et Cosmochimica Acta, 2009. **73**(16): p. 4824-4835.
102. Cozzarelli, I.M., et al., *Geochemical and microbiological methods for evaluating anaerobic processes in an aquifer contaminated by landfill leachate*. Environmental science & technology, 2000. **34**(18): p. 4025-4033.
103. Truche, L., et al., *Kinetics of pyrite to pyrrhotite reduction by hydrogen in calcite buffered solutions between 90 and 180°C: Implications for nuclear waste disposal*. Geochimica et Cosmochimica Acta, 2010. **74**(10): p. 2894-2914.
104. Hall, A., *Pyrite-pyrrhotine redox reactions in nature*. Mineralogical Magazine, 1986. **50**(356): p. 223-229.
105. Truche, L., et al., *Sulphide mineral reactions in clay-rich rock induced by high hydrogen pressure. Application to disturbed or natural settings up to 250°C and 30bar*. Chemical Geology, 2013. **351**: p. 217-228.
106. Wiltowski, T., et al., *Kinetics and mechanisms of iron sulfide reductions in hydrogen and in carbon monoxide*. Journal of Solid State Chemistry, 1987. **71**(1): p. 95-102.
107. Lambert, J., G. Simkovich, and P. Walker, *The kinetics and mechanism of the pyrite-to-pyrrhotite transformation*. Metallurgical and materials transactions B, 1998. **29**(2): p. 385-396.
108. Didier, M., et al., *Adsorption of Hydrogen Gas and Redox Processes in Clays*. Environmental Science & Technology, 2012. **46**(6): p. 3574-3579.

109. Moslemi, H., P. Shamsi, and F. Habashi, *Pyrite and pyrrhotite open circuit potentials study: Effects on flotation*. Minerals Engineering, 2011. **24**(10): p. 1038-1045.
110. Jozwiak, W.K., et al., *Reduction behavior of iron oxides in hydrogen and carbon monoxide atmospheres*. Applied Catalysis A: General, 2007. **326**(1): p. 17-27.
111. Munteanu, G., L. Ilieva, and D. Andreeva, *Kinetic parameters obtained from TPR data for α -Fe₂O₃ and Au α -Fe₂O₃ systems*. Thermochemica Acta, 1997. **291**(1-2): p. 171-177.
112. Lin, H.-Y., Y.-W. Chen, and C. Li, *The mechanism of reduction of iron oxide by hydrogen*. Thermochemica Acta, 2003. **400**(1-2): p. 61-67.
113. Lebedeva, O.E. and W.M. Sachtler, *Enhanced reduction of Fe₂O₃ caused by migration of TM ions out of zeolite channels*. Journal of Catalysis, 2000. **191**(2): p. 364-372.
114. Turkdogan, E. and J. Vinters, *Gaseous reduction of iron oxides: Part I. Reduction of hematite in hydrogen*. Metallurgical and Materials Transactions B, 1971. **2**(11): p. 3175-3188.
115. Monazam, E.R., R.W. Breault, and R. Siriwardane, *Kinetics of hematite to wustite by hydrogen for chemical looping combustion*. Energy & Fuels, 2014. **28**(8): p. 5406-5414.
116. Iglauer, S., M. Ali, and A. Keshavarz, *Hydrogen Wettability of Sandstone Reservoirs: Implications for Hydrogen Geo-Storage*. Geophysical Research Letters, 2021. **48**(3): p. e2020GL090814.
117. Zeng, L., et al., *Interpreting Water Uptake by Shale with Ion Exchange, Surface Complexation, and Disjoining Pressure*. Energy & Fuels, 2019. **33**(9): p. 8250-8258.
118. Zeng, L., et al., *Wettability alteration induced water uptake in shale oil reservoirs: A geochemical interpretation for oil-brine-OM interaction during hydraulic fracturing*. International Journal of Coal Geology, 2019. **213**: p. 103277.
119. Chalbaud, C., et al., *Interfacial tension measurements and wettability evaluation for geological CO₂ storage*. Advances in water resources, 2009. **32**(1): p. 98-109.
120. Farokhpoor, R., et al., *Wettability behaviour of CO₂ at storage conditions*. International Journal of Greenhouse Gas Control, 2013. **12**: p. 18-25.
121. Arif, M., et al., *CO₂ storage in carbonates: Wettability of calcite*. International Journal of Greenhouse Gas Control, 2017. **62**: p. 113-121.
122. Kaveh, N.S., A. Barnhoorn, and K.-H. Wolf, *Wettability evaluation of silty shale caprocks for CO₂ storage*. International Journal of Greenhouse Gas Control, 2016. **49**: p. 425-435.
123. Iglauer, S., *CO₂-water-rock wettability: variability, influencing factors, and implications for CO₂ geostorage*. Accounts of chemical research, 2017. **50**(5): p. 1134-1142.
124. Higgs, S., et al., *In-situ hydrogen wettability characterisation for underground hydrogen storage*. International Journal of Hydrogen Energy, 2022. **47**(26): p. 13062-13075.
125. Yekta, A.E., et al., *Determination of Hydrogen-Water Relative Permeability and Capillary Pressure in Sandstone: Application to Underground Hydrogen Injection in Sedimentary Formations*. Transport in Porous Media, 2018. **122**(2): p. 333-356.
126. Hosseini, M., et al., *Hydrogen wettability of carbonate formations: Implications for hydrogen geo-storage*. Journal of Colloid and Interface Science, 2022.

127. Zeng, L., et al., *Hydrogen wettability in carbonate reservoirs: Implication for underground hydrogen storage from geochemical perspective*. International Journal of Hydrogen Energy, 2022.
128. Esfandyari, H., et al., *Experimental evaluation of rock mineralogy on hydrogen-wettability: Implications for hydrogen geo-storage*. Journal of Energy Storage, 2022. **52**: p. 104866.
129. Ali, M., et al., *Assessment of wettability and rock-fluid interfacial tension of caprock: Implications for hydrogen and carbon dioxide geo-storage*. International Journal of Hydrogen Energy, 2022. **47**(30): p. 14104-14120.
130. Ali, M., et al., *Influence of pressure, temperature and organic surface concentration on hydrogen wettability of caprock; implications for hydrogen geo-storage*. Energy Reports, 2021. **7**: p. 5988-5996.
131. Raza, A., et al., *Injunctivity and quantification of capillary trapping for CO₂ storage: A review of influencing parameters*. Journal of Natural Gas Science and Engineering, 2015. **26**: p. 510-517.
132. Zhou, Y., D.G. Hatzignatiou, and J.O. Helland, *On the estimation of CO₂ capillary entry pressure: Implications on geological CO₂ storage*. International journal of greenhouse gas control, 2017. **63**: p. 26-36.
133. Hosseini, M., et al., *H₂- brine interfacial tension as a function of salinity, temperature, and pressure; implications for hydrogen geo-storage*. Journal of Petroleum Science and Engineering, 2022. **213**: p. 110441.
134. Chow, Y.T.F., G.C. Maitland, and J.P.M. Trusler, *Interfacial tensions of the (CO₂+N₂+H₂O) system at temperatures of (298 to 448)K and pressures up to 40MPa*. The Journal of Chemical Thermodynamics, 2016. **93**: p. 392-403.
135. Pan, B., X. Yin, and S. Iglauer, *Rock-fluid interfacial tension at subsurface conditions: Implications for H₂, CO₂ and natural gas geo-storage*. International Journal of Hydrogen Energy, 2021. **46**(50): p. 25578-25585.
136. Yekeen, N., et al., *Clay-hydrogen and clay-cushion gas interfacial tensions: Implications for hydrogen storage*. International Journal of Hydrogen Energy, 2022. **47**(44): p. 19155-19167.
137. Carroll, S.A. and J.V. Walther, *Kaolinite dissolution at 25 degrees, 60 degrees, and 80 degrees C*. American Journal of Science, 1990. **290**(7): p. 797-810.
138. Ganor, J., J.L. Mogollón, and A.C. Lasaga, *The effect of pH on kaolinite dissolution rates and on activation energy*. Geochimica et Cosmochimica Acta, 1995. **59**(6): p. 1037-1052.
139. De Lucia, M., et al., *Measurements of H₂ solubility in saline solutions under reservoir conditions: preliminary results from project H₂STORE*. Energy Procedia, 2015. **76**: p. 487-494.
140. Pokrovsky, O.S., et al., *Calcite, dolomite and magnesite dissolution kinetics in aqueous solutions at acid to circumneutral pH, 25 to 150 C and 1 to 55 atm pCO₂: New constraints on CO₂ sequestration in sedimentary basins*. Chemical geology, 2009. **265**(1-2): p. 20-32.
141. Shao, H., et al., *In situ spectrophotometric determination of pH under geologic CO₂ sequestration conditions: method development and application*. Environmental science & technology, 2013. **47**(1): p. 63-70.
142. Shao, H., C.J. Thompson, and K.J. Cantrell, *Evaluation of experimentally measured and model-calculated pH for rock-brine-CO₂ systems under geologic CO₂ sequestration conditions*. Chemical Geology, 2013. **359**: p. 116-124.

143. Jacquemet, N. *Hydrogen reactivity with an aquifer-PHREEQC geochemical thermodynamics calculations*. in *27e édition de la Réunion des Sciences de la Terre*. 2021.
144. Truche, L., et al., *Kinetics of pyrite to pyrrhotite reduction by hydrogen in calcite buffered solutions between 90 and 180 C: Implications for nuclear waste disposal*. *Geochimica et Cosmochimica Acta*, 2010. **74**(10): p. 2894-2914.
145. Suslow, T.V., *Oxidation-reduction potential (ORP) for water disinfection monitoring, control, and documentation*. 2004.
146. VanLoon, G.W. and S.J. Duffy, *Environmental chemistry: a global perspective*. 2017: Oxford university press.
147. Ugarte, E.R. and S. Salehi, *A review on well integrity issues for underground hydrogen storage*. *Journal of Energy Resources Technology*, 2022. **144**(4).
148. Kiran, R., et al., *Identification and evaluation of well integrity and causes of failure of well integrity barriers (A review)*. *Journal of Natural Gas Science and Engineering*, 2017. **45**: p. 511-526.
149. ISO, N., *Petroleum and natural gas industries-Well integrity-Part 1: Life cycle governance*. 2017, International Standard Geneva.
150. Peukert, S., *Cementy powszechnego użytku i specjalne*. Polski Cement sp. z oo, Kraków, 2000.
151. Szabó-Krausz, Z., et al., *Wellbore cement alteration during decades of abandonment and following CO2 attack—A geochemical modelling study in the area of potential CO2 reservoirs in the Pannonian Basin*. *Applied Geochemistry*, 2020. **113**: p. 104516.
152. Pernites, R.B. and A.K. Santra, *Portland cement solutions for ultra-high temperature wellbore applications*. *Cement and Concrete Composites*, 2016. **72**: p. 89-103.
153. Hussain, A., et al. *Experimental Investigation of Wellbore Integrity of Depleted Oil and Gas Reservoirs for Underground Hydrogen Storage*. in *Offshore Technology Conference*. 2022. OnePetro.
154. Jacquemet, N., P. Chiquet, and A. Grauls. *Hydrogen reactivity with (1) a well cement-PHREEQC geochemical thermodynamics calculations*. in *1st Geoscience & Engineering in Energy Transition Conference*. 2020. European Association of Geoscientists & Engineers.
155. Dopffel, N., S. Jansen, and J. Gerritse, *Microbial side effects of underground hydrogen storage—knowledge gaps, risks and opportunities for successful implementation*. *International Journal of Hydrogen Energy*, 2021. **46**(12): p. 8594-8606.
156. Simon, J., A.M. Ferriz, and L.C. Correias, *HyUnder – Hydrogen Underground Storage at Large Scale: Case Study Spain*. *Energy Procedia*, 2015. **73**: p. 136-144.
157. Kruck, O., et al., *Assessment of the potential, the actors and relevant business cases for large scale and seasonal storage of renewable electricity by hydrogen underground storage in Europe*. KBB Undergr. Technol. GmbH, 2013.
158. Bauer, S., *Underground Sun.Storage*. 2017.
159. Schippers, A., F. Glombitza, and W. Sand, *Geobiotechnology II Energy Resources*. *Subsurface Technologies, Organic Pollutants and Mining Legal Principles*, nd< <http://www.springer.com/series/10>, 2014.
160. Gniese, C., et al., *Relevance of Deep-Subsurface Microbiology for Underground Gas Storage and Geothermal Energy Production*, in *Geobiotechnology II: Energy Resources, Subsurface Technologies, Organic Pollutants and Mining Legal Principles*, A. Schippers, F. Glombitza, and W. Sand, Editors. 2014, Springer Berlin Heidelberg: Berlin, Heidelberg. p. 95-121.
161. Ebrahimiyejta, A., *Characterization of geochemical interactions and migration of hydrogen in sandstone sedimentary formations: application to geological storage*. 2017, Université d'Orléans.

162. Stolten, D. and B. Emonts, *Hydrogen Science and Engineering, 2 Volume Set: Materials, Processes, Systems, and Technology*. Vol. 1. 2016: John Wiley & Sons.
163. Pérez, A., et al. *Patagonia wind-hydrogen project: underground storage and methanation*. in *21st world hydrogen energy conference*. 2016.
164. Pedersen, K., *Subterranean microbial populations metabolize hydrogen and acetate under in situ conditions in granitic groundwater at 450 m depth in the Äspö Hard Rock Laboratory, Sweden*. FEMS microbiology ecology, 2012. **81**(1): p. 217-229.
165. Gregory, S.P., et al., *Subsurface microbial hydrogen cycling: natural occurrence and implications for industry*. Microorganisms, 2019. **7**(2): p. 53.
166. Bagnoud, A., et al., *Reconstructing a hydrogen-driven microbial metabolic network in Opalinus Clay rock*. Nature Communications, 2016. **7**(1): p. 1-10.
167. Thiyagarajan, S.R., et al., *A comprehensive review of the mechanisms and efficiency of underground hydrogen storage*. Journal of Energy Storage, 2022. **51**: p. 104490.
168. Davey, M.E., et al., *Microbial selective plugging of sandstone through stimulation of indigenous bacteria in a hypersaline oil reservoir*. Geomicrobiology Journal, 1998. **15**(4): p. 335-352.
169. Martin, D., et al., *Carbonate precipitation under pressure for bioengineering in the anaerobic subsurface via denitrification*. Environmental science & technology, 2013. **47**(15): p. 8692-8699.
170. Tang, C.-S., et al., *Factors affecting the performance of microbial-induced carbonate precipitation (MICP) treated soil: a review*. Environmental Earth Sciences, 2020. **79**(5): p. 1-23.
171. Lewandowski, Z. and H. Beyenal, *Mechanisms of microbially influenced corrosion*, in *Marine and industrial biofouling*. 2009, Springer. p. 35-64.
172. Bai, P., et al., *Initiation and developmental stages of steel corrosion in wet H₂S environments*. Corrosion Science, 2015. **93**: p. 109-119.
173. Videla, H.A. and L.K. Herrera, *Understanding microbial inhibition of corrosion. A comprehensive overview*. International Biodeterioration & Biodegradation, 2009. **63**(7): p. 896-900.
174. Thaysen, E.M., et al., *Estimating microbial growth and hydrogen consumption in hydrogen storage in porous media*. Renewable and Sustainable Energy Reviews, 2021. **151**: p. 111481.
175. Lankof, L. and R. Tarkowski, *Assessment of the potential for underground hydrogen storage in bedded salt formation*. International Journal of Hydrogen Energy, 2020. **45**(38): p. 19479-19492.
176. Caglayan, D.G., et al., *Technical potential of salt caverns for hydrogen storage in Europe*. International Journal of Hydrogen Energy, 2020. **45**(11): p. 6793-6805.
177. Teatini, P., et al., *Geomechanical response to seasonal gas storage in depleted reservoirs: A case study in the Po River basin, Italy*. Journal of Geophysical Research: Earth Surface, 2011. **116**(F2).
178. Nicol, A., et al., *Fault permeability and CO₂ storage*. Energy Procedia, 2017. **114**: p. 3229-3236.
179. Zheng, D., et al., *Key evaluation techniques in the process of gas reservoir being converted into underground gas storage*. Petroleum Exploration and Development, 2017. **44**(5): p. 840-849.
180. McGrath, A.G. and I. Davison, *Damage zone geometry around fault tips*. Journal of Structural Geology, 1995. **17**(7): p. 1011-1024.
181. Gudmundsson, A., *Active fault zones and groundwater flow*. Geophysical Research Letters, 2000. **27**(18): p. 2993-2996.

182. Paul, P.K., M.D. Zoback, and P.H. Hennings. *Fluid flow in a fractured reservoir using a geomechanically-constrained fault zone damage model for reservoir simulation*. in *SPE Annual Technical Conference and Exhibition*. 2007. OnePetro.
183. White, A.J., M.O. Traugott, and R.E. Swarbrick, *The use of leak-off tests as means of predicting minimum in-situ stress*. *Petroleum Geoscience*, 2002. **8**(2): p. 189-193.
184. Lin, W., et al., *Estimation of minimum principal stress from an extended leak-off test onboard the Chikyu drilling vessel and suggestions for future test procedures*. *Scientific drilling*, 2008. **6**: p. 43-47.
185. Michihiro, K., T. Fujiwara, and H. Yoshioka. *Study on estimating geostresses by the Kaiser effect of AE*. in *The 26th US Symposium on Rock Mechanics (USRMS)*. 1985. OnePetro.
186. Holcomb, D.J. *General theory of the Kaiser effect*. in *International Journal of Rock Mechanics and Mining Sciences & Geomechanics Abstracts*. 1993. Elsevier.
187. Moeck, I., G. Kwiatak, and G. Zimmermann, *Slip tendency analysis, fault reactivation potential and induced seismicity in a deep geothermal reservoir*. *Journal of Structural Geology*, 2009. **31**(10): p. 1174-1182.
188. Chengyuan, X., et al., *Structural failure mechanism and strengthening method of fracture plugging zone for lost circulation control in deep naturally fractured reservoirs*. *Petroleum Exploration and Development*, 2020. **47**(2): p. 430-440.
189. Kamali, A. and A. Ghassemi, *Analysis of injection-induced shear slip and fracture propagation in geothermal reservoir stimulation*. *Geothermics*, 2018. **76**: p. 93-105.
190. Gong, F., et al., *Evaluation of shear strength parameters of rocks by preset angle shear, direct shear and triaxial compression tests*. *Rock Mechanics and Rock Engineering*, 2020. **53**(5): p. 2505-2519.
191. Chang, S.-H. and C.-I. Lee, *Estimation of cracking and damage mechanisms in rock under triaxial compression by moment tensor analysis of acoustic emission*. *International Journal of Rock Mechanics and Mining Sciences*, 2004. **41**(7): p. 1069-1086.
192. Fredrich, J.T., et al., *Geomechanical modeling of reservoir compaction, surface subsidence, and casing damage at the Belridge diatomite field*. *SPE Reservoir Evaluation & Engineering*, 2000. **3**(04): p. 348-359.
193. Li, L., et al., *Numerical simulation of 3D hydraulic fracturing based on an improved flow-stress-damage model and a parallel FEM technique*. *Rock Mechanics and rock engineering*, 2012. **45**(5): p. 801-818.
194. Wang, X., et al., *The developmental characteristics of natural fractures and their significance for reservoirs in the Cambrian Niutitang marine shale of the Sangzhi block, southern China*. *Journal of Petroleum Science and Engineering*, 2018. **165**: p. 831-841.
195. Zoback, M.D., et al. *The importance of slow slip on faults during hydraulic fracturing stimulation of shale gas reservoirs*. in *SPE Americas Unconventional Resources Conference*. 2012. OnePetro.
196. Handin, J., *On the Coulomb-Mohr failure criterion*. *Journal of Geophysical Research*, 1969. **74**(22): p. 5343-5348.
197. Simon, A. and A.J. Collison, *Pore-water pressure effects on the detachment of cohesive streambeds: seepage forces and matric suction*. *Earth Surface Processes and Landforms*, 2001. **26**(13): p. 1421-1442.
198. Suppe, J., *Absolute fault and crustal strength from wedge tapers*. *Geology*, 2007. **35**(12): p. 1127-1130.
199. Sibson, R.H., *An assessment of field evidence for 'Byerlee' friction*. *Pure and Applied Geophysics*, 1994. **142**(3): p. 645-662.

200. Samuelson, J. and C.J. Spiers, *Fault friction and slip stability not affected by CO₂ storage: Evidence from short-term laboratory experiments on North Sea reservoir sandstones and caprocks*. International Journal of Greenhouse Gas Control, 2012. **11**: p. S78-S90.
201. Yao, Q., et al., *Mechanisms of failure in coal samples from underground water reservoir*. Engineering Geology, 2020. **267**: p. 105494.
202. Bakker, E., et al., *Frictional behaviour and transport properties of simulated fault gouges derived from a natural CO₂ reservoir*. International Journal of Greenhouse Gas Control, 2016. **54**: p. 70-83.
203. Scibek, J., *Multidisciplinary database of permeability of fault zones and surrounding protolith rocks at world-wide sites*. Scientific Data, 2020. **7**(1): p. 95.
204. Rezaee, R., *Fundamentals of gas shale reservoirs*. 2015: John Wiley & Sons.
205. Saffer, D.M., *The permeability of active subduction plate boundary faults*. Geofluids, 2015. **15**(1-2): p. 193-215.
206. Mizoguchi, K., et al., *Internal structure and permeability of the Nojima fault, southwest Japan*. Journal of Structural Geology, 2008. **30**(4): p. 513-524.
207. Evans, J.P., C.B. Forster, and J.V. Goddard, *Permeability of fault-related rocks, and implications for hydraulic structure of fault zones*. Journal of structural Geology, 1997. **19**(11): p. 1393-1404.
208. Gan, Q. and D. Elsworth, *Analysis of fluid injection -induced fault reactivation and seismic slip in geothermal reservoirs*. Journal of Geophysical Research: Solid Earth, 2014. **119**(4): p. 3340-3353.
209. Mondelli, C., et al., *Hydrogen adsorption and diffusion in synthetic Na-montmorillonites at high pressures and temperature*. International Journal of Hydrogen Energy, 2015. **40**(6): p. 2698-2709.
210. Zeng, L., et al., *Role of brine composition on rock surface energy and its implications for subcritical crack growth in calcite*. Journal of Molecular Liquids, 2020. **303**: p. 112638.
211. Lu, Y., et al., *Analytical modelling of wettability alteration-induced micro-fractures during hydraulic fracturing in tight oil reservoirs*. Fuel, 2019. **249**: p. 434-440.
212. Røyne, A., K.N. Dalby, and T. Hassenkam, *Repulsive hydration forces between calcite surfaces and their effect on the brittle strength of calcite - bearing rocks*. Geophysical Research Letters, 2015. **42**(12): p. 4786-4794.
213. Røyne, A., J. Bisschop, and D.K. Dysthe, *Experimental investigation of surface energy and subcritical crack growth in calcite*. Journal of Geophysical Research: Solid Earth, 2011. **116**(B4).
214. Zeng, L., et al., *Effect of fluid-shale interactions on shales micromechanics: Nanoindentation experiments and interpretation from geochemical perspective*. Journal of Natural Gas Science and Engineering, 2022. **101**: p. 104545.
215. Zeng, L., et al., *Effect of fluid saturation and salinity on sandstone rock weakening: experimental investigations and interpretations from physicochemical perspective*. Acta Geotechnica, 2022.
216. Zeng, L., et al., *Interpreting micromechanics of fluid-shale interactions with geochemical modelling and disjoining pressure: Implications for calcite-rich and quartz-rich shales*. Journal of Molecular Liquids, 2020: p. 114117.
217. Atkinson, B.K., *Subcritical crack growth in geological materials*. Journal of Geophysical Research: Solid Earth, 1984. **89**(B6): p. 4077-4114.
218. Rostom, F., et al., *Effect of fluid salinity on subcritical crack propagation in calcite*. Tectonophysics, 2013. **583**: p. 68-75.

219. Xu, M., A. Gupta, and H. Dehghanpour, *How significant are strain and stress induced by water imbibition in dry gas shales?* Journal of Petroleum Science and Engineering, 2019. **176**: p. 428-443.
220. Griffith, A.A., VI. *The phenomena of rupture and flow in solids*. Philosophical transactions of the royal society of london. Series A, containing papers of a mathematical or physical character, 1921. **221**(582-593): p. 163-198.
221. Bergsaker, A.S., et al., *The effect of fluid composition, salinity, and acidity on subcritical crack growth in calcite crystals*. Journal of Geophysical Research: Solid Earth, 2016. **121**(3): p. 1631-1651.
222. Chen, X., P. Eichhubl, and J.E. Olson, *Effect of water on critical and subcritical fracture properties of Woodford shale*. Journal of Geophysical Research: Solid Earth, 2017. **122**(4): p. 2736-2750.
223. Aderibigbe, A.A. and R.H. Lane, *Rock/Fluid Chemistry Impacts on Shale Fracture Behavior*, in *SPE International Symposium on Oilfield Chemistry*. 2013, Society of Petroleum Engineers: The Woodlands, Texas, USA. p. 10.
224. Dehghanpour, H., et al., *Spontaneous Imbibition of Brine and Oil in Gas Shales: Effect of Water Adsorption and Resulting Microfractures*. Energy & Fuels, 2013. **27**(6): p. 3039-3049.
225. Leung, D.Y., G. Caramanna, and M.M. Maroto-Valer, *An overview of current status of carbon dioxide capture and storage technologies*. Renewable and Sustainable Energy Reviews, 2014. **39**: p. 426-443.
226. Meredith, P. and B. Atkinson, *Fracture toughness and subcritical crack growth during high-temperature tensile deformation of Westerly granite and Black gabbro*. Physics of the Earth and Planetary Interiors, 1985. **39**(1): p. 33-51.
227. Nara, Y., et al., *Effects of relative humidity and temperature on subcritical crack growth in igneous rock*. International Journal of Rock Mechanics and Mining Sciences, 2010. **47**(4): p. 640-646.
228. Eppes, M.C. and R. Keanini, *Mechanical weathering and rock erosion by climate -dependent subcritical cracking*. Reviews of Geophysics, 2017. **55**(2): p. 470-508.
229. Mathias, S.A., et al., *Analytical solution for Joule–Thomson cooling during CO₂ geo-sequestration in depleted oil and gas reservoirs*. International Journal of Greenhouse Gas Control, 2010. **4**(5): p. 806-810.
230. Oldenburg, C.M., *Screening and ranking framework for geologic CO₂ storage site selection on the basis of health, safety, and environmental risk*. Environmental Geology, 2008. **54**(8): p. 1687-1694.
231. Ziabakhsh-Ganji, Z. and H. Kooi, *Sensitivity of Joule–Thomson cooling to impure CO₂ injection in depleted gas reservoirs*. Applied energy, 2014. **113**: p. 434-451.
232. Jamaloei, B.Y. and K. Asghari, *The Joule-Thomson Effect in Petroleum Fields: II. CO₂ Sequestration, Wellbore Temperature Profiles, and Thermal Stresses and Wellbore Stability*. Energy Sources, Part A: Recovery, Utilization, and Environmental Effects, 2015. **37**(3): p. 236-244.
233. Yadali Jamaloei, B. and K. Asghari, *The Joule-Thomson Effect in Petroleum Fields: I. Well Testing, Multilateral/Slanted Wells, Hydrate Formation, and Drilling/Completion/Production Operations*. Energy Sources, Part A: Recovery, Utilization, and Environmental Effects, 2015. **37**(2): p. 217-224.
234. Rutqvist, J., *The geomechanics of CO₂ storage in deep sedimentary formations*. Geotechnical and Geological Engineering, 2012. **30**(3): p. 525-551.
235. Jeanne, P., Y. Zhang, and J. Rutqvist, *Influence of hysteretic stress path behavior on seal integrity during gas storage operation in a depleted reservoir*. Journal of Rock Mechanics and Geotechnical Engineering, 2020. **12**(4): p. 886-899.

236. Day, J.W., et al., *Life cycle of oil and gas fields in the Mississippi River Delta: a review*. Water, 2020. **12**(5): p. 1492.
237. Atan, S., et al. *The viability of gas injection EOR in Eagle Ford shale reservoirs*. in *SPE Annual Technical Conference and Exhibition*. 2018. OnePetro.
238. Schimmel, M., S. Hangx, and C. Spiers, *Impact of chemical environment on compaction behaviour of quartz sands during stress-cycling*. Rock Mechanics and Rock Engineering, 2021. **54**(3): p. 981-1003.
239. Sun, J., et al., *Injection–production mechanisms and key evaluation technologies for underground gas storages rebuilt from gas reservoirs*. Natural Gas Industry B, 2018. **5**(6): p. 616-622.
240. Edge, J., *Hydrogen adsorption and dynamics in clay minerals*. 2015, UCL (University College London).
241. Lord, A.S., *Overview of geologic storage of natural gas with an emphasis on assessing the feasibility of storing hydrogen*. 2009, Sandia National Laboratories (SNL), Albuquerque, NM, and Livermore, CA
242. Masood, E. and J. Tollefson, '*COP26 hasn't solved the problem*': scientists react to UN climate deal. Nature, 2021. **599**(7885): p. 355-356.
243. Mountford, H., et al., *COP26: Key Outcomes From the UN Climate Talks in Glasgow*.
244. Martins, F., et al., *Analysis of fossil fuel energy consumption and environmental impacts in European countries*. Energies, 2019. **12**(6): p. 964.
245. Shen, C., et al., *Consequence assessment of high-pressure hydrogen storage tank rupture during fire test*. Journal of Loss Prevention in the Process Industries, 2018. **55**: p. 223-231.
246. Zheng, J., et al., *Development of high pressure gaseous hydrogen storage technologies*. International Journal of Hydrogen Energy, 2012. **37**(1): p. 1048-1057.
247. Aceves, S.M., J. Martinez-Frias, and O. Garcia-Villazana, *Analytical and experimental evaluation of insulated pressure vessels for cryogenic hydrogen storage*. International Journal of Hydrogen Energy, 2000. **25**(11): p. 1075-1085.
248. Aceves, S.M., et al., *High-density automotive hydrogen storage with cryogenic capable pressure vessels*. International Journal of Hydrogen Energy, 2010. **35**(3): p. 1219-1226.
249. Sakintuna, B., F. Lamari-Darkrim, and M. Hirscher, *Metal hydride materials for solid hydrogen storage: a review*. International journal of hydrogen energy, 2007. **32**(9): p. 1121-1140.
250. Alapati, S.V., J.K. Johnson, and D.S. Sholl, *Using first principles calculations to identify new destabilized metal hydride reactions for reversible hydrogen storage*. Physical Chemistry Chemical Physics, 2007. **9**(12): p. 1438-1452.
251. Bobbitt, N.S., J. Chen, and R.Q. Snurr, *High-throughput screening of metal–organic frameworks for hydrogen storage at cryogenic temperature*. The Journal of Physical Chemistry C, 2016. **120**(48): p. 27328-27341.
252. Modisha, P.M., et al., *The prospect of hydrogen storage using liquid organic hydrogen carriers*. Energy & fuels, 2019. **33**(4): p. 2778-2796.
253. Mehranfar, A., M. Izadyar, and A.A. Esmaeili, *Hydrogen storage by N-ethylcarbazol as a new liquid organic hydrogen carrier: A DFT study on the mechanism*. International Journal of Hydrogen Energy, 2015. **40**(17): p. 5797-5806.
254. Cheng, H.-M., Q.-H. Yang, and C. Liu, *Hydrogen storage in carbon nanotubes*. Carbon, 2001. **39**(10): p. 1447-1454.
255. Seenithurai, S., et al., *Al-decorated carbon nanotube as the molecular hydrogen storage medium*. international journal of hydrogen energy, 2014. **39**(23): p. 11990-11998.

256. Kanaani, M., B. Sedaei, and M. Asadian-Pakfar, *Role of Cushion Gas on Underground Hydrogen Storage in Depleted Oil Reservoirs*. *Journal of Energy Storage*, 2022. **45**: p. 103783.
257. Jackson, R.B., *The integrity of oil and gas wells*. *Proceedings of the National Academy of Sciences*, 2014. **111**(30): p. 10902-10903.

Preprint Under Review